

A shape optimization approach for electrical impedance tomography with point measurements

Yuri Flores Albuquerque*

Antoine Laurain*

Kevin Sturm†

Abstract

Working within the class of piecewise constant conductivities, the inverse problem of electrical impedance tomography can be recast as a shape optimization problem where the discontinuity interface is the unknown. Using Gröger's W_p^1 -estimates for mixed boundary value problems, the averaged adjoint method is extended to the case of Banach spaces, which allows to compute the derivative of shape functionals involving point evaluations. We compute the corresponding distributed expression of the shape derivative and show that it may contain Dirac measures in addition to the usual domain integrals. We use this distributed shape derivative to devise a numerical algorithm, show various numerical results supporting the method, and based on these results we discuss the influence of the point measurements patterns on the quality of the reconstructions.

Mathematics Subject Classification. 49Q10, 35Q93, 35R30, 35R05

1 Introduction

Electrical impedance tomography (EIT) is a low cost, noninvasive, radiation free and portable imaging modality with various applications in medical imaging, geophysics, civil engineering and nondestructive testing. In particular, it is an active field of research in medical imaging, where devices based on EIT are already used in practice, with applications to lung imaging such as diagnosis of pulmonary embolism [19], monitoring patients undergoing mechanical ventilation, breast imaging, acute cerebral stroke, or cardiac activity monitoring; we refer to the reviews [8, 12] and the references therein.

Two mathematical models for EIT have been actively investigated over the last few decades. The *continuum model* has been widely studied in the case where applied currents and voltage measurements are supposed to be known on the entire boundary. This model is closely related to the *Calderón problem*, which has attracted the attention of a large community of mathematicians in the last decades; see [8, 12]. It consists in determining the uniqueness and stability properties of the conductivity reconstruction when the full Dirichlet-to-Neumann map is known, which corresponds, roughly speaking, to the availability of an infinite amount of applied currents and boundary measurements.

Despite its usefulness, the continuum model is not realistic for applications, indeed, in the case of medical imaging for instance, it does not take into account the fact that currents are applied through electrodes attached by small patches to the patient, and that voltage measurements are also performed through these electrodes. Therefore, the applied currents and voltage measurements are available only on a subset of the boundary. In the literature, this situation is referred to as *partial measurements* as opposed to *full measurements* for the standard Calderón problem. This leads to the more realistic *electrode model* [58], which also takes into account the electro-chemical reaction occurring at the interface between the electrode and the skin.

As the field of EIT is growing more mature, the awareness of these restrictions has increased also among mathematicians. As a consequence, the study of the continuum model with partial boundary data has attracted much attention in the recent years. Uniqueness results with partial boundary data in dimension $n \geq 3$ were obtained in [46], in [49] for C^2 -conductivities, and in [51] for $W^{3/2+\delta, 2n}$ -conductivities with $\delta > 0$. Uniqueness results were extended to conductivities of class $C^{1,\infty}(\overline{\Omega}) \cap H^{3/2}(\Omega)$

*Instituto de Matemática e Estatística, Universidade de São Paulo, Rua do Matão 1010, 05508-090, São Paulo, Brazil (yuri.falbu@gmail.com, laurain@ime.usp.br)

†Technische Universität Wien, Institut für Analysis und Scientific Computing, Wiedner Hauptstraße 8-10, 1040 Wien, Austria (kevin.sturm@asc.tuwien.ac.at)

and conductivities in $W^{1,\infty}(\Omega) \cap H^{3/2+\delta}(\Omega)$ with $0 < \delta < 1/2$ arbitrarily small but fixed in [52]. We refer to [48] for a review of theoretical results on the Calderón problem with partial data. Regarding numerical methods, sparsity priors are used to improve the reconstruction using partial data in [26, 27]. D-bar methods in two dimensions were investigated in [5, 38] and resistor networks in [13].

Due to the small size of the electrodes compared to the rest of the boundary in many practical applications, the idea of modeling small electrodes by point electrodes using Dirac measures is appealing from the mathematical standpoint. This point of view has been introduced as a *point electrode model* and justified in [33]; see also [15, 42, 43]. We also observe that mathematical models using point measurements are highly relevant for large-scale inverse problems such as full-waveform inversion where the dimensions of the receivers are several orders of magnitude smaller than the dimensions of the physical domain of the model; see [63].

The problem of reconstructing conductivities presenting sharp interfaces in EIT, also known as the inclusion detection problem, has attracted significant interest in the last three decades, starting from the pioneering works [24, 25]. Several numerical methods have been developed for reconstructing discontinuous conductivities including the factorization method introduced in [14, 50]; see also the review [34], monotonicity-based shape reconstructions [28, 35, 36], the enclosure method for reconstructing the convex hull of a set of inclusions [44, 45], the MUSIC algorithm for determining the locations of small inclusions [7], a nonlinear integral equation method [22], and topological derivative-based methods [6, 11, 40, 41]. Shape optimization techniques, which are the basis of the present paper, have also been employed to tackle this problem: based on level set methods [16, 54], for a polygonal partition of the domain [9], using second-order shape sensitivity [3], and using a single boundary measurement [2, 39].

In this framework, the conductivity is assumed to be piecewise constant or piecewise smooth, and it is then convenient to reformulate the problem as a shape optimization problem [57] in order to investigate the sensitivity with respect to perturbations of a trial interface. This sensitivity analysis relies on the calculation of the *shape derivative*, which can be written either in a strong form, usually as a boundary integral, or in a weak form which often presents itself as a domain integral involving the derivative of the perturbation field. The usefulness of the weak form of the shape derivative, often called *domain expression* or *distributed shape derivative*, is known since the pioneering works [20, 37] but has been seldom used since then in comparison with the boundary expression. A revival of the distributed shape derivative has been observed since [10], and this approach has been further developed in the context of EIT and level set methods in [54], see also [29].

An important contribution of the present paper is to extend the framework developed in [54] to the case of point measurements in EIT. The main issue for shape functionals involving point evaluations is that one needs the continuity of the state, for which the usual H^1 -regularity in two dimensions is insufficient. Functionals with point evaluations and pointwise constraints have been studied intensively in the optimal control literature; see [32, 62]. In particular, a convenient idea from optimal control is to use Gröger's W_p^1 -estimates [30, 31] with $p > 2$ to obtain continuity of the state in two dimensions. Here, we adapt this idea in the context of shape optimization and of the averaged adjoint method, in the spirit of [61]. We show that in general the shape derivative contains Dirac measures, and that the adjoint state is slightly less regular than H^1 due to the presence of Dirac measures on the right-hand side. Another important contribution of this paper is to investigate the relations between the domain and boundary expressions of the shape derivative depending on the interface regularity, and the minimal regularity of the interface for which the boundary expression of the shape derivative can be obtained in the context of EIT with point measurements.

We start by recalling in Section 2 the W_p^1 -estimates for mixed boundary value problems introduced in [30]. We then formulate in Section 3 the shape optimization approach for the inverse problem of EIT and show how the averaged adjoint method can be adapted to the context of Banach spaces. Then, we compute the distributed shape derivative and prove its validity for a conductivity inclusion which is only open. When the inclusion is Lipschitz polygonal or C^1 , we also obtain the boundary expression of the shape derivative. Finally, in Section 4 we explain the numerical algorithm based on the distributed shape derivative and we present a set of results showing the efficiency of the approach. Introducing an error measure for the reconstruction, we also discuss the quality of reconstructions depending on the number of point measurements, applied boundary currents and noise level. More details about the averaged adjoint method are given in an appendix for the sake of completeness.

2 Preliminaries

2.1 Mixed boundary value problems in W_p^1

In this section we recall the framework introduced in [30] for obtaining a W_p^1 -estimate for solutions to mixed boundary value problems for second order elliptic PDEs.

Definition 2.1 (see [30, 32]). Let $\mathcal{D} \subset \mathbb{R}^2$ and $\Gamma \subset \partial\mathcal{D}$ be given. We say that $\mathcal{D} \cup \Gamma$ is regular (in the sense of Gröger) if \mathcal{D} is a bounded Lipschitz domain, Γ is a relatively open part of the boundary $\partial\mathcal{D}$, $\Gamma_0 := \partial\mathcal{D} \setminus \Gamma$ has positive measure, and Γ_0 is a finite union of closed and nondegenerated (i.e., not a single point) curved pieces of $\partial\mathcal{D}$.

Let \mathcal{D}, Γ and Γ_0 be as in Definition 2.1 and define for $d \geq 1$:

$$\mathcal{C}_\Gamma^\infty(\mathcal{D}, \mathbb{R}^d) := \{f|_{\mathcal{D}} \mid f \in \mathcal{C}^\infty(\mathbb{R}^2, \mathbb{R}^d), \text{supp } f \cap \Gamma_0 = \emptyset\}.$$

In the scalar case, i.e. for $d = 1$, we write $\mathcal{C}_\Gamma^\infty(\mathcal{D})$ instead of $\mathcal{C}_\Gamma^\infty(\mathcal{D}, \mathbb{R})$ and use a similar notation for the other function spaces. We denote by $W_p^1(\mathcal{D})$, $1 \leq p \leq \infty$ the Sobolev space of weakly differentiable functions with weak derivative in $L^p(\mathcal{D})$. For $p, p' \geq 1$ satisfying $\frac{1}{p} + \frac{1}{p'} = 1$, we define the Sobolev space

$$W_{\Gamma,p}^1(\mathcal{D}, \mathbb{R}^d) := \overline{\mathcal{C}_\Gamma^\infty(\mathcal{D}, \mathbb{R}^d)}^{W_p^1},$$

where W_p^1 stands for the usual norm in $W^{1,p}(\mathcal{D}, \mathbb{R}^d)$, and the dual space

$$W_{\Gamma,p}^{-1}(\mathcal{D}, \mathbb{R}^d) := (W_{\Gamma,p'}^1(\mathcal{D}, \mathbb{R}^d))^*.$$

We use the notation id for the identity function in \mathbb{R}^2 , and \mathbb{I} for the 2×2 identity matrix.

Let $2 \leq q < \infty$ and $1 \leq q' \leq 2$ satisfying $\frac{1}{q} + \frac{1}{q'} = 1$. Let $\mathbb{A} \in L^\infty(\mathcal{D})^{2 \times 2}$ be a matrix-valued function satisfying for all $\eta, \theta \in \mathbb{R}^2$ and $x \in \overline{\mathcal{D}}$:

$$\mathbb{A}(x)\theta \cdot \theta \geq m|\theta|^2 \text{ and } |\mathbb{A}(x)\eta| \leq M|\eta|, \text{ with } m > 0 \text{ and } M > 0, \quad (1)$$

where $|\cdot|$ denotes the Euclidean norm and $m \leq M$. Introduce

$$\begin{aligned} a : W_{\Gamma,q}^1(\mathcal{D}) \times W_{\Gamma,q'}^1(\mathcal{D}) &\rightarrow \mathbb{R} \\ (v, w) &\mapsto \int_{\mathcal{D}} \mathbb{A} \nabla v \cdot \nabla w. \end{aligned}$$

Then, define the corresponding operator

$$\begin{aligned} \mathcal{A}_q : W_{\Gamma,q}^1(\mathcal{D}) &\rightarrow W_{\Gamma,q}^{-1}(\mathcal{D}), \\ v &\mapsto \mathcal{A}_q v := a(v, \cdot). \end{aligned} \quad (2)$$

Let \mathcal{P} be defined by, for $u, v \in W_{\Gamma,2}^1(\mathcal{D})$,

$$\langle \mathcal{P}u, v \rangle := \int_{\mathcal{D}} \nabla u \cdot \nabla v + uv.$$

By Hölder's inequality it follows that $\mathcal{P} : W_{\Gamma,p}^1(\mathcal{D}) \rightarrow W_{\Gamma,p}^{-1}(\mathcal{D})$ is a well-defined and continuous operator for all $p \geq 2$. We also introduce the constant

$$M_p := \sup\{\|v\|_{W_p^1(\mathcal{D})} \mid v \in W_{\Gamma,p}^1(\mathcal{D}), \|\mathcal{P}v\|_{W_{\Gamma,p}^{-1}(\mathcal{D})} \leq 1\}.$$

It is easily verified that $M_2 = 1$. Now we define the set of regular domains in the sense of Gröger

$$\Xi := \{(\mathcal{D}, \Gamma) \mid \mathcal{D} \subset \mathbb{R}^2, \Gamma \subset \partial\mathcal{D}, \text{ and } \mathcal{D} \cup \Gamma \text{ is regular}\}.$$

Definition 2.2. Denote by R_q , $2 \leq q < \infty$, the set of regular domains $(\mathcal{D}, \Gamma) \in \Xi$ for which \mathcal{P} maps $W_{\Gamma,q}^1(\mathcal{D})$ onto $W_{\Gamma,q}^{-1}(\mathcal{D})$.

Then we have the following results from [31, Lemma 1].

Lemma 2.3. *Let $(\mathcal{D}, \Gamma) \in R_q$ for some $q > 2$. Then $(\mathcal{D}, \Gamma) \in R_p$ for $2 \leq p \leq q$ and $M_p \leq M_q^\theta$ if $\frac{1}{p} = \frac{1-\theta}{2} + \frac{\theta}{q}$.*

We can now state an adapted version of [31, Theorem 1] which plays a key role in our investigations.

Theorem 2.4. *[31, Theorem 1] Let $(\mathcal{D}, \Gamma) \in R_{q_0}$ for some $q_0 > 2$. Suppose that \mathbb{A} satisfies assumptions (1) for q_0 and let \mathcal{A}_q be defined by (2). Then $\mathcal{A}_q : W_{\Gamma,q}^1(\mathcal{D}) \rightarrow W_{\Gamma,q}^{-1}(\mathcal{D})$ is an isomorphism provided that $q \in [2, q_0]$ and $M_q k < 1$, where $k := (1 - m^2/M^2)^{1/2}$, and*

$$\|\mathcal{A}_q^{-1}\|_{L(W_{\Gamma,q}^{-1}(\mathcal{D}), W_{\Gamma,q}^1(\mathcal{D}))} \leq c_q, \quad (3)$$

where $c_q := mM^{-2}M_q(1 - M_q k)^{-1}$. Finally, $M_q k < 1$ is satisfied if

$$\frac{1}{q} > \frac{1}{2} - \left(\frac{1}{2} - \frac{1}{q_0} \right) \frac{|\log k|}{\log M_{q_0}}.$$

Remark 2.5. • If $(\mathcal{D}, \Gamma) \in R_q$, then $M_q < \infty$.

- For every regular $(\mathcal{D}, \Gamma) \in \Xi$, there exists a $q_0 > 2$ so that $(\mathcal{D}, \Gamma) \in R_{q_0}$; cf [30, Theorem 3].
- For sufficiently small $q > 2$, the constant c_q in (3) can be chosen to be independent of q ; see [61, Corollary 5].

We now explain how a particular case of the theory described above can be applied to our problem. Let $\sigma \in L^\infty(\mathcal{D})$ satisfying pointwise a.e. $\bar{\sigma} \geq \sigma \geq \underline{\sigma} > 0$ where $\bar{\sigma}, \underline{\sigma} > 0$ are constants. It is clear that $\mathbb{A} := \sigma \mathbb{I} \in L^\infty(\mathcal{D})^{2 \times 2}$ satisfies assumptions (1). In view of Remark 2.5, there exists $q_0 > 2$ such that $(\mathcal{D}, \Gamma) \in R_{q_0}$. For $q \in [2, q_0]$, $f \in L^q(\mathcal{D})$ and $g \in L^\infty(\partial\mathcal{D})$, the functional

$$\langle F, v \rangle := \int_{\mathcal{D}} f v + \int_{\Gamma} g v, \quad v \in W_{\Gamma,q}^1(\mathcal{D})$$

defines an element in $(W_{\Gamma,q'}^1(\mathcal{D}))^* = W_{\Gamma,q}^{-1}(\mathcal{D})$. Therefore, it follows from Theorem 2.4 that there is a unique $u \in W_{\Gamma,q}^1(\mathcal{D})$ solution to

$$\int_{\mathcal{D}} \sigma \nabla u \cdot \nabla v = \int_{\mathcal{D}} f v + \int_{\Gamma} g v \quad \text{for all } v \in W_{\Gamma,q'}^1(\mathcal{D}),$$

provided $q \in [2, q_0]$ is sufficiently close to 2.

2.2 Shape optimization framework

In this section, we recall basic notions about first and second order Eulerian shape derivatives. For $k \geq 0$ we define

$$\mathcal{C}_c^k(\mathcal{D}, \mathbb{R}^2) := \{V \in \mathcal{C}^k(\mathcal{D}, \mathbb{R}^2) \mid V \text{ has compact support in } \mathcal{D}\},$$

and $\mathcal{C}_c^\infty(\mathcal{D}, \mathbb{R}^2)$ similarly, and we equip these spaces with their usual topologies; see [1, 1.56, pp. 19-20]. Consider a vector field $V \in \mathcal{C}_c^1(\mathcal{D}, \mathbb{R}^2)$ and the associated flow $T_t : \mathcal{D} \rightarrow \mathcal{D}$, $t \in [0, t_0]$ defined for each $x_0 \in \mathcal{D}$ as $T_t(x_0) := x(t)$, where $x : [0, t_0] \rightarrow \mathbb{R}^d$ solves

$$\dot{x}(t) = V(x(t)) \quad \text{for } t \in [0, t_0], \quad x(0) = x_0. \quad (4)$$

Let $\mathbb{P}(\mathcal{D})$ be the set of all open sets compactly contained in \mathcal{D} , where $\mathcal{D} \subset \mathbb{R}^2$ is assumed to be open and bounded. For $\Omega \in \mathbb{P}(\mathcal{D})$, we consider the family of perturbed domains

$$\Omega_t := T_t(\Omega). \quad (5)$$

Definition 2.6 (Shape derivative). Let $J : \mathbb{P}(\mathcal{D}) \rightarrow \mathbb{R}$ be a shape functional.

- (i) The Eulerian semiderivative of J at Ω in direction $V \in \mathcal{C}_c^1(\mathcal{D}, \mathbb{R}^2)$ is defined by, when the limit exists,

$$dJ(\Omega)(V) := \lim_{t \searrow 0} \frac{J(\Omega_t) - J(\Omega)}{t}. \quad (6)$$

- (ii) J is said to be *shape differentiable* at Ω if it has a Eulerian semiderivative at Ω for all $V \in \mathcal{C}_c^\infty(\mathcal{D}, \mathbb{R}^2)$ and the mapping

$$dJ(\Omega) : \mathcal{C}_c^\infty(\mathcal{D}, \mathbb{R}^2) \rightarrow \mathbb{R}, \quad V \mapsto dJ(\Omega)(V)$$

is linear and continuous, in which case $dJ(\Omega)(V)$ is called the *Eulerian shape derivative* at Ω , or simply *shape derivative* at Ω .

3 EIT with point measurements

3.1 Problem formulation

Let $\mathcal{D} \cup \Gamma \in \Xi$ (see Definition 2.1) and $\Omega \in \mathbb{P}(\mathcal{D})$. Denote $\Omega^c := \mathcal{D} \setminus \Omega$ and $\Omega_t^c := T_t(\Omega^c)$. In this section, n denotes the outward unit normal vector to Ω . Introduce the conductivity $\sigma_\Omega = \sigma_1 \chi_\Omega + \sigma_0 \chi_{\Omega^c}$ with (σ_0, σ_1) positive scalars, $\sigma_1 > \sigma_0$, and $f_\Omega = f_1 \chi_\Omega + f_0 \chi_{\Omega^c}$ where $f_0, f_1 \in H^1(\mathcal{D})$. Here, χ_Ω denotes the characteristic function of Ω . Let $p > 2$ and $1 < p' < 2$ satisfying $\frac{1}{p} + \frac{1}{p'} = 1$. In view of the development in Section 2.1, $u \in W_{\Gamma, p}^1(\Omega)$ is the solution to the mixed boundary value problem

$$\int_{\mathcal{D}} \sigma_\Omega \nabla u \cdot \nabla v = \int_{\mathcal{D}} f_\Omega v + \int_{\Gamma} g v \quad \text{for all } v \in W_{\Gamma, p'}^1(\mathcal{D}), \quad (7)$$

with $g \in L^\infty(\partial\mathcal{D})$. Observe that u depends on Ω through σ_Ω .

In EIT, g represents an input, in this case an electric current applied on the boundary, and u is the corresponding potential. Then, measurements h of the potential on a subset Γ_h of $\overline{\mathcal{D}}$ are performed. Given the Cauchy data (g, h) , the task is to find the best possible approximation of the unknown shape Ω . To obtain a better reconstruction, we apply several input currents g_i , $i = 1, \dots, I$, and the corresponding measurements are denoted by h_i . Assuming (σ_0, σ_1) are known and denoting u_i the solution of (7) with $g = g_i$, the EIT problem becomes then:

$$\text{given } \{(g_i, h_i)\}_{i=1}^I, \text{ find } \Omega \text{ such that } u_i = h_i \text{ on } \Gamma_h \text{ for } i = 1, \dots, I. \quad (8)$$

However, (8) is idealized since in practice the measurements h_i are corrupted by noise, therefore we cannot expect that $u_i = h_i$ be exactly achievable, but rather that $|u_i - h_i|$ should be minimized. When Γ_h is a manifold of one or two dimensions, a common approach is to minimize an appropriate cost functional such as

$$J(\Omega) = \frac{1}{2} \sum_{i=1}^I \int_{\Gamma_h} (u_i - h_i)^2. \quad (9)$$

Another popular approach is to use a Kohn-Vogelius type functional; see [54].

In this paper we are interested in the case where $\Gamma_h = \{x_k\}_{k=1}^K \in \overline{\mathcal{D}}$ is a finite set of points, i.e. we only have a finite collection of point measurements. In this case, a Kohn-Vogelius type functional does not seem appropriate since we would need h on all of $\partial\mathcal{D}$ for this approach. The functional (9) on the other hand can be adapted to the case $\Gamma_h = \{x_k\}_{k=1}^K$ in the following way. For $i = 1, \dots, I$, assume that measurements $\{h_i(x_k)\}_{k=1}^K \in \mathbb{R}^K$ are available. For $\Omega \in \mathbb{P}(\mathcal{D})$ and $x_0 \in \overline{\mathcal{D}}$, we consider the shape functional

$$J(\Omega) := \frac{1}{2} \sum_{i=1}^I \mu_i \sum_{k=1}^K \delta_{x_k} ((u_i - h_i)^2) = \frac{1}{2} \sum_{i=1}^I \mu_i \sum_{k=1}^K (u_i(x_k) - h_i(x_k))^2, \quad (10)$$

where $\delta_{x_k} : \mathcal{C}(\overline{\mathcal{D}}) \rightarrow \mathbb{R}$ is the Dirac measure concentrated at x_k and μ_i are given constants. Note that in view of the continuous embedding $W_{\Gamma, p}^1(\mathcal{D}) \subset \mathcal{C}(\overline{\mathcal{D}})$ for $p > 2$ in two dimensions, the point evaluation

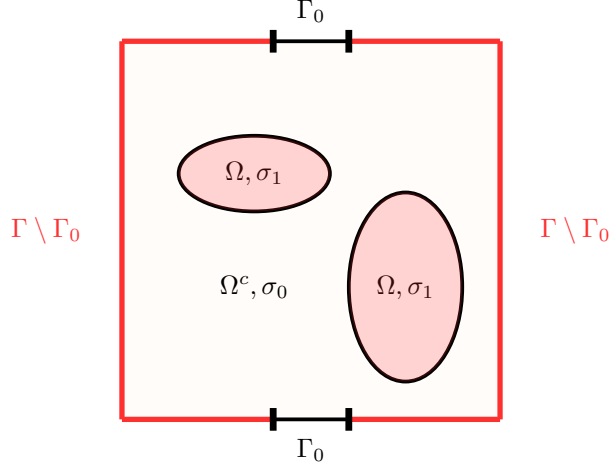


Figure 1: Partition $\mathcal{D} = \Omega \cup \Omega^c$.

of u_i in (10) is well-defined. Without loss of generality, we will compute the shape derivative for the simpler case $I = 1$ and $\mu_1 = 1$, in which case the cost functional becomes

$$J(\Omega) = \frac{1}{2} \sum_{k=1}^K \delta_{x_k} ((u - h)^2) = \frac{1}{2} \sum_{k=1}^K (u(x_k) - h(x_k))^2. \quad (11)$$

The formula of the shape derivative in the general case (10) can then be obtained by summation.

3.2 Shape derivative

For $\Omega \in \mathbb{P}(\mathcal{D})$ and $V \in \mathcal{C}_c^1(\mathcal{D}, \mathbb{R}^2)$, define Ω_t as in (5). Since V has compact support in \mathcal{D} , we have $\Omega_t \subset \mathcal{D}$ for all $t \in [0, t_0]$. Now we consider the Lagrangian $\mathcal{L} : \mathbb{P}(\mathcal{D}) \times W_{\Gamma, p}^1(\mathcal{D}) \times W_{\Gamma, p'}^1(\mathcal{D}) \rightarrow \mathbb{R}$ associated with the cost functional (11) and the PDE constraint (7) defined by

$$\mathcal{L}(\Omega, \varphi, \psi) := \frac{1}{2} \sum_{k=1}^K (\varphi(x_k) - h(x_k))^2 + \int_{\mathcal{D}} \sigma_{\Omega} \nabla \varphi \cdot \nabla \psi - f_{\Omega} \psi - \int_{\Gamma} g \psi. \quad (12)$$

Aiming at applying the averaged adjoint method [60], we introduce the *shape-Lagrangian* $G : [0, t_0] \times W_{\Gamma, p}^1(\mathcal{D}) \times W_{\Gamma, p'}^1(\mathcal{D}) \rightarrow \mathbb{R}$ as

$$\begin{aligned} G(t, \varphi, \psi) &:= \mathcal{L}(\Omega_t, \varphi \circ T_t^{-1}, \psi \circ T_t^{-1}) \\ &= \frac{1}{2} \sum_{k=1}^K (\varphi \circ T_t^{-1} - h)^2(x_k) + \int_{\mathcal{D}} \sigma_{\Omega_t} \nabla(\varphi \circ T_t^{-1}) \cdot \nabla(\psi \circ T_t^{-1}) - f_{\Omega_t} \psi \circ T_t^{-1} - \int_{\Gamma} g \psi \circ T_t^{-1}, \end{aligned}$$

see Appendix 1 for a detailed explanation. Notice that for all $p \geq 1$ we have $\varphi \in W_{\Gamma, p}^1(\mathcal{D})$ if and only if $\varphi \circ T_t \in W_{\Gamma, p}^1(\mathcal{D})$; see [64, Theorem 2.2.2, p. 52]. Observe that

$$\begin{aligned} \sigma_{\Omega_t} \circ T_t &= \sigma_1 \chi_{\Omega_t} \circ T_t + \sigma_0 \chi_{\Omega_t^c} \circ T_t = \sigma_1 \chi_{\Omega} + \sigma_0 \chi_{\Omega^c} = \sigma_{\Omega}, \\ f_{\Omega_t} \circ T_t &= f_1 \circ T_t \chi_{\Omega_t} \circ T_t + f_0 \circ T_t \chi_{\Omega_t^c} \circ T_t = f_1 \circ T_t \chi_{\Omega} + f_0 \circ T_t \chi_{\Omega^c}, \end{aligned}$$

and we introduce the function $f^t := f_1 \circ T_t \chi_{\Omega} + f_0 \circ T_t \chi_{\Omega^c}$.

Using the fact that $T_t = \text{id}$ on $\partial \mathcal{D}$ and proceeding with the change of variables $x \mapsto T_t(x)$ inside the integrals in $G(t, \varphi, \psi)$, we obtain using the chain rule

$$G(t, \varphi, \psi) = \frac{1}{2} \sum_{k=1}^K (\varphi \circ T_t^{-1} - h)^2(x_k) + \int_{\mathcal{D}} \sigma_{\Omega} A(t) \nabla \varphi \cdot \nabla \psi - f^t \psi - \int_{\Gamma} g \psi, \quad (13)$$

where $A(t) := \det(DT_t)DT_t^{-1}DT_t^{-\top}$.

For $t \in [0, t_0]$, let us define the perturbation \mathcal{A}_q^t of \mathcal{A}_q defined in (2) as follows:

$$\begin{aligned} \mathcal{A}_q^t : W_{\Gamma,q}^1(\mathcal{D}) &\rightarrow W_{\Gamma,q}^{-1}(\mathcal{D}), \\ v &\mapsto \left(w \mapsto \langle \mathcal{A}_q^t v, w \rangle := \int_{\mathcal{D}} \sigma_{\Omega} A(t) \nabla v \cdot \nabla w \right). \end{aligned} \quad (14)$$

By continuity of $t \mapsto A(t) : [0, t_0] \rightarrow C(\overline{\mathcal{D}})^{2 \times 2}$, for every $\epsilon > 0$ there exists $\delta > 0$ so that the following result (see [61, Lemma 13]) follows immediately:

$$A(t)(x) \eta \cdot \eta \geq (1 - \epsilon) |\eta|^2 \quad \text{for all } \eta \in \mathbb{R}^2 \text{ and all } (t, x) \in [0, \delta] \times \overline{\mathcal{D}}, \quad (15)$$

$$|A(t)(x)| \leq 1 + \epsilon \quad \text{for all } (t, x) \in [0, \delta] \times \overline{\mathcal{D}}. \quad (16)$$

The continuity properties (15)-(16) imply the following perturbed version of Theorem 2.4.

Lemma 3.1. *For each $(\mathcal{D}, \Gamma) \in \Xi$ there exists $q_0 > 2$, $\epsilon > 0$ and $\delta > 0$ so that for all $t \in [0, \delta]$ and all $q \in [2, q_0]$ satisfying $M_q k < 1$, where $k := (1 - m^2/M^2)^{1/2} < 1$ with $m = \underline{\sigma}(1 - \epsilon)$ and $M = \overline{\sigma}(1 + \epsilon)$, the mapping $\mathcal{A}_q^t : W_{\Gamma,q}^1(\mathcal{D}) \rightarrow W_{\Gamma,q}^{-1}(\mathcal{D})$ defined by (14) is an isomorphism. Moreover, we have for all $t \in [0, \delta]$ that*

$$\|(\mathcal{A}_q^t)^{-1}\|_{L(W_{\Gamma,q}^{-1}(\mathcal{D}), W_{\Gamma,q}^1(\mathcal{D}))} \leq c_q, \quad (17)$$

where $c_q := mM^{-2}M_q(1 - M_q k)^{-1}$ is independent of t . Finally, $M_q k < 1$ is satisfied if

$$\frac{1}{q} > \frac{1}{2} - \left(\frac{1}{2} - \frac{1}{q_0} \right) \frac{|\log k|}{\log M_{q_0}}.$$

Proof. We have $\overline{\sigma} \geq \sigma \geq \underline{\sigma} > 0$ with $\underline{\sigma} := \min\{\sigma_0, \sigma_1\}$, $\overline{\sigma} := \max\{\sigma_0, \sigma_1\}$ and $\underline{\sigma} < \overline{\sigma}$. Let us choose $\epsilon < 1$ and δ such that (15),(16) is satisfied, and let $t \in [0, \delta]$. In view of (15),(16) it immediately follows that $\mathbb{A} = \sigma_{\Omega} A(t) \in L^{\infty}(\mathcal{D})^{2 \times 2}$ satisfies assumptions (1) with $m := \underline{\sigma}(1 - \epsilon)$ and $M := \overline{\sigma}(1 + \epsilon)$. Hence, the result follows directly from Theorem 2.4, since M and m are independent of t . \square

The main statement of this section is the following theorem.

Theorem 3.2 (distributed shape derivative). *Let $\mathcal{D} \cup \Gamma \subset \mathbb{R}^2$ be a regular domain in the sense of Gröger and $\Omega \in \mathbb{P}(\mathcal{D})$. Assume that $\Gamma_h \cap \partial\Omega = \emptyset$ and $f_{\Omega} = f_1 \chi_{\Omega} + f_0 \chi_{\Omega^c}$ where $f_0, f_1 \in H^1(\mathcal{D})$. Then the shape derivative of J at Ω in direction $V \in \mathcal{C}_c^1(\mathcal{D}, \mathbb{R}^2)$ is given by*

$$dJ(\Omega)(V) = \mathbf{S}_0(V) + \int_{\mathcal{D}} \mathbf{S}_1 : DV, \quad (18)$$

where $\mathbf{S}_1 \in L^1(\mathcal{D})^{2 \times 2}$ and $\mathbf{S}_0 \in (\mathcal{C}^0(\overline{\mathcal{D}}, \mathbb{R}^2))^*$ are defined by

$$\mathbf{S}_1 = -2\sigma_{\Omega} \nabla u \odot \nabla p + (\sigma_{\Omega} \nabla u \cdot \nabla p - fp) \mathbb{I}, \quad (19)$$

$$\mathbf{S}_0(V) = \mathbf{S}_0^s(V) + \int_{\mathcal{D}} \mathbf{S}_0^r \cdot V \quad (20)$$

$$\mathbf{S}_0^r = -p \tilde{\nabla} f \quad (21)$$

$$\mathbf{S}_0^s = - \sum_{k=1}^K \left((u - h) \nabla u \right) (x_k) \delta_{x_k}, \quad (22)$$

where $\nabla u \odot \nabla p := (\nabla u \otimes \nabla p + \nabla p \otimes \nabla u)/2$, $\tilde{\nabla} f := \nabla f_1 \chi_{\Omega} + \nabla f_0 \chi_{\Omega^c}$ and $\mathbf{S}_0^r \in L^1(\mathcal{D}, \mathbb{R}^2)$.

Also, there exists $q > 2$ such that the adjoint $p \in W_{\Gamma,q}^1(\mathcal{D})$ is the solution to

$$\int_{\mathcal{D}} \sigma_{\Omega} \nabla p \cdot \nabla \varphi = - \sum_{k=1}^K (u(x_k) - h(x_k)) \varphi(x_k) \quad \text{for all } \varphi \in W_{\Gamma,q}^1(\mathcal{D}). \quad (23)$$

Proof. We employ the averaged adjoint approach of [60], we refer to Appendix 1 for details about the method. We closely follow the argumentation of [61]. Let us define the perturbed state $u^t \in W_{\Gamma,q}^1(\mathcal{D})$ solution of

$$\int_{\mathcal{D}} \sigma_{\Omega} A(t) \nabla u^t \cdot \nabla \varphi = \int_{\mathcal{D}} f^t \varphi + \int_{\Gamma} g \varphi \quad \text{for all } \varphi \in W_{\Gamma,q'}^1(\mathcal{D}). \quad (24)$$

The mapping $F_t : W_{\Gamma,q'}^1(\mathcal{D}) \rightarrow \mathbb{R}$ defined by

$$\langle F_t, v \rangle := \int_{\mathcal{D}} f^t v + \int_{\Gamma} g v \quad \text{for } v \in W_{\Gamma,q'}^1(\mathcal{D})$$

is well-defined and continuous. Consequently, thanks to Theorem 2.4 there is a unique solution to (24) in $W_{\Gamma,q}^1(\mathcal{D})$ for $q > 2$ sufficiently close to 2. Using (17) we get

$$\|u^t\|_{W_{\Gamma,q}^1(\mathcal{D})} \leq c_q \|F_t\|_{W_{\Gamma,q}^{-1}(\mathcal{D})} \leq C(\|f^t\|_{L^2(\mathcal{D})} + \|g\|_{L^\infty(\partial\mathcal{D})}).$$

It follows that for some constant C independent of t , we have

$$\|u^t\|_{W_{\Gamma,q}^1(\mathcal{D})} \leq C. \quad (25)$$

Following (47), the *averaged adjoint equation* reads: find $p^t \in W_{\Gamma,q}^1(\mathcal{D})$, such that

$$\int_0^1 d_{\varphi} G(t, su^t + (1-s)u^0; p^t)(\varphi) ds = 0 \quad \text{for all } \varphi \in W_{\Gamma,q}^1(\mathcal{D}), \quad (26)$$

which is equivalent to, using the fact that $A(t)^T = A(t)$,

$$\begin{aligned} & \int_{\mathcal{D}} \sigma_{\Omega} A(t) \nabla p^t \cdot \nabla \varphi \\ &= \frac{1}{2} \sum_{k=1}^K (u^t \circ T_t^{-1}(x_k) + u^0 \circ T_t^{-1}(x_k) - 2h(x_k)) \varphi \circ T_t^{-1}(x_k) \quad \text{for all } \varphi \in W_{\Gamma,q}^1(\mathcal{D}). \end{aligned} \quad (27)$$

Let us introduce the adjoint operator

$$\begin{aligned} (\mathcal{A}_q^t)^* : W_{\Gamma,q}^{-1}(\mathcal{D})^* &= W_{\Gamma,q'}^1(\mathcal{D}) \rightarrow W_{\Gamma,q}^1(\mathcal{D})^* = W_{\Gamma,q'}^{-1}(\mathcal{D}), \\ w &\mapsto (v \mapsto \langle (\mathcal{A}_q^t)^* w, v \rangle := \langle w, \mathcal{A}_q^t v \rangle). \end{aligned} \quad (28)$$

Using (14) and the fact that $A(t)^T = A(t)$ we get for $w \in W_{\Gamma,q'}^1(\mathcal{D})$ and $v \in W_{\Gamma,q}^1(\mathcal{D})$,

$$\langle (\mathcal{A}_q^t)^* w, v \rangle = \int_{\mathcal{D}} \sigma_{\Omega} A(t) \nabla w \cdot \nabla v.$$

Now, in view of Lemma 3.1 there exists $q > 2$ and $\delta > 0$ such that the mapping $\mathcal{A}_q^t : W_{\Gamma,q}^1(\mathcal{D}) \rightarrow W_{\Gamma,q}^{-1}(\mathcal{D})$ is an isomorphism for all $t \in [0, \delta]$. Thus, the adjoint mapping $(\mathcal{A}_q^t)^* : W_{\Gamma,q'}^1(\mathcal{D}) \rightarrow W_{\Gamma,q}^{-1}(\mathcal{D})$ is also an isomorphism.

Now the functional $R_t : W_{\Gamma,q}^1(\mathcal{D}) \rightarrow \mathbb{R}$ defined by

$$\langle R_t, v \rangle := \frac{1}{2} \sum_{k=1}^K (u^t \circ T_t^{-1}(x_k) + u^0 \circ T_t^{-1}(x_k) - 2h(x_k)) v \circ T_t^{-1}(x_k) \quad \text{for } v \in W_{\Gamma,q}^1(\mathcal{D}).$$

is well-defined and continuous. Therefore, since $(\mathcal{A}_q^t)^*$ is an isomorphism, the averaged adjoint equation $(\mathcal{A}_q^t)^* p^t = R_t$ has a unique solution $p^t \in W_{\Gamma,q'}^1(\mathcal{D})$.

Using the continuous embedding of $W_{\Gamma,q}^1(\mathcal{D})$ into the space of continuous functions $\mathcal{C}(\overline{\mathcal{D}})$ for $q > 2$ in two dimensions, it also follows that

$$\begin{aligned} \|p^t\|_{W_{\Gamma,q'}^1(\mathcal{D})} &\leq C \max_{k \in \{1, \dots, K\}} |(u^t \circ T_t^{-1} + u^0 \circ T_t^{-1} - 2h)(x_k)| \\ &\leq C \left(\|u^t\|_{W_{\Gamma,q}^1(\mathcal{D})} + \|u^0\|_{W_{\Gamma,q}^1(\mathcal{D})} + \max_{k \in \{1, \dots, K\}} |h(x_k)| \right). \end{aligned}$$

Then using (25) we get, for some constant C independent of t ,

$$\|p^t\|_{W_{\Gamma,q'}^1(\mathcal{D})} \leq C. \quad (29)$$

With the estimate (29) we readily verify that $p^t \rightharpoonup p^0$ weakly in $W_{\Gamma,q'}^1(\mathcal{D})$ as $t \searrow 0$. Using (48) we have

$$\frac{G(t, u^t, p^t) - G(0, u^0, p^0)}{t} = \frac{G(t, u^0, p^t) - G(0, u^0, p^t)}{t} \quad (30)$$

and then in view of (13)

$$\begin{aligned} \frac{G(t, u^0, p^t) - G(0, u^0, p^t)}{t} &= \frac{1}{2} \sum_{k=1}^K \frac{(u^0 \circ T_t^{-1} - h)^2(x_k) - (u^0 - h)^2(x_k)}{t} \\ &\quad + \int_{\mathcal{D}} \sigma_{\Omega} \frac{A(t) - \mathbb{I}}{t} \nabla u^0 \cdot \nabla p^t - \frac{f^t - f^0}{t} p^t. \end{aligned} \quad (31)$$

Using the assumption $\Gamma_h \cap \partial\Omega = \emptyset$, we have for all $k = 1, \dots, K$ that x_k belongs either to Ω , to $\mathcal{D} \setminus \overline{\Omega}$ or to $\partial\mathcal{D}$. Assume first that x_k belongs either to Ω or to $\mathcal{D} \setminus \overline{\Omega}$. Since σ_{Ω} is constant in Ω and in $\mathcal{D} \setminus \overline{\Omega}$, u is harmonic in these sets, therefore using elliptic regularity results we have $u \in \mathcal{C}^{\infty}(B(x_k, r_k))$ for sufficiently small r_k , where $B(x_k, r_k)$ denotes the open ball of center x_k and radius r_k . Thus, the first term on the right hand side of (31) converges as $t \searrow 0$. Now if $x_k \in \partial\mathcal{D}$, then $T_t(x_k) = x_k$ due to $V \in \mathcal{C}_c^1(\mathcal{D}, \mathbb{R}^2)$, and the first term on the right hand side of (31) is equal to zero, so we obtain the same formula as in the case $x_k \in \mathcal{D} \setminus \overline{\Omega}$. Also, using $V \in \mathcal{C}_c^1(\mathcal{D}, \mathbb{R}^2)$ we have the following convergence properties (see [47, Lem. 3.1] and [59, Lemma 2.16])

$$\frac{A(t) - I}{t} \rightarrow A'(0) := \operatorname{div}(V) - DV - DV^{\top} \quad \text{strongly in } \mathcal{C}(\overline{\mathcal{D}})^{2 \times 2}, \quad (32)$$

$$\frac{f^t - f^0}{t} \rightarrow \tilde{f}'(0) := f_{\Omega} \operatorname{div}(V) + \tilde{\nabla} f \cdot V \quad \text{strongly in } L^2(\mathcal{D}), \quad (33)$$

and we conclude that the right hand side of (31) converges to

$$-\sum_{k=1}^K (u^0 - h)(x_k) \nabla u^0(x_k) \cdot V(x_k) + \int_{\mathcal{D}} \sigma_{\Omega} A'(0) \nabla u^0 \cdot \nabla p^0 - \tilde{f}'(0) p^0. \quad (34)$$

In view of (13) this shows

$$\lim_{t \searrow 0} \frac{G(t, u^t, p^t) - G(0, u^0, p^0)}{t} = \partial_t G(0, u^0, p^0), \quad (35)$$

which shows that Assumption 5.2 is satisfied. Using tensor calculus, it is then readily verified that (34) can be brought into expression (18). The regularity $\mathbf{S}_1 \in L^1(\mathcal{D})^{2 \times 2}$ is due to $u \in W_{\Gamma,q}^1(\mathcal{D})$, and $p \in W_{\Gamma,q'}^1(\mathcal{D})$ and the regularity of \mathbf{S}_0^r is a consequence of the regularity of p and f_{Ω} . \square

An interesting feature of Theorem 3.2 is to show that the distributed shape derivative exists when Ω is only open. Another relevant issue is to determine the minimal regularity of Ω for which we can obtain the boundary expression of the shape derivative. The rest of this section is devoted to the study of this question. We start with the following well-known result which describes the structure of the boundary expression of the shape derivative; see [21, pp. 480-481].

Theorem 3.3 (Zolésio's structure theorem). *Let Ω be open with $\partial\Omega$ compact and of class \mathcal{C}^{k+1} , $k \geq 0$. Assume J has a Eulerian shape derivative at Ω and $dJ(\Omega)$ is continuous for the $\mathcal{C}^k(\mathcal{D}, \mathbb{R}^d)$ -topology. Then, there exists a linear and continuous functional $l : \mathcal{C}^k(\partial\Omega) \rightarrow \mathbb{R}$ such that*

$$dJ(\Omega)(V) = l(V|_{\partial\Omega} \cdot n) \quad \text{for all } V \in \mathcal{C}_c^k(\mathcal{D}, \mathbb{R}^d). \quad (36)$$

Theorem 3.3 requires Ω to be at least C^1 , however we show in Proposition 3.4 that even for Lipschitz domains one can obtain a boundary expression for the shape derivative, see (40), even though we get a weaker structure than (36) since the tangential component of V may be present in (40). Recall that a bounded domain is called Lipschitz if it is locally representable as the graph of a Lipschitz function. In this case, it is well-known that the surface measure is well-defined on $\partial\Omega$ and there exists an outward pointing normal vector n at almost every point on $\partial\Omega$; see [23, Section 4.2, p. 127].

In the rest of the paper, the exponents $+$ and $-$ denote the restrictions of functions to Ω and to $\mathcal{D} \setminus \bar{\Omega}$, respectively, and the notation $\llbracket \phi \rrbracket := \phi^+|_{\partial\Omega} - \phi^-|_{\partial\Omega}$ denotes the jump across the interface $\partial\Omega$ of a given function ϕ .

Proposition 3.4. *Suppose that $\Gamma_h \cap \partial\Omega = \emptyset$, $\Omega \in \mathbb{P}(\mathcal{D})$ and $V \in \mathcal{C}_c^1(\mathcal{D} \setminus \Gamma_h, \mathbb{R}^2)$, then we have*

$$\operatorname{div}(\mathbf{S}_1^+) = (\mathbf{S}_0^r)^+ \quad \text{a.e. in } \Omega \setminus \Gamma_h, \quad (37)$$

$$\operatorname{div}(\mathbf{S}_1^-) = (\mathbf{S}_0^r)^- \quad \text{a.e. in } (\mathcal{D} \setminus \bar{\Omega}) \setminus \Gamma_h. \quad (38)$$

If $\mathbf{S}_1^+ \in W^{1,1}(\Omega, \mathbb{R}^{2 \times 2})$ and $\mathbf{S}_1^- \in W^{1,1}(\mathcal{D} \setminus \bar{\Omega}, \mathbb{R}^{2 \times 2})$, then

$$dJ(\Omega)(V) = \int_{\Omega} \operatorname{div}(\mathbf{S}_1^T V) + \int_{\mathcal{D} \setminus \bar{\Omega}} \operatorname{div}(\mathbf{S}_1^T V). \quad (39)$$

If in addition Ω is Lipschitz, we also have the boundary expression

$$dJ(\Omega)(V) = \int_{\partial\Omega} \llbracket \mathbf{S}_1 \rrbracket n \cdot V. \quad (40)$$

If in addition Ω is of class C^1 , we obtain the boundary expression

$$dJ(\Omega)(V) = \int_{\partial\Omega} (\llbracket \mathbf{S}_1 \rrbracket n \cdot n) V \cdot n. \quad (41)$$

Proof. In view of [54, Theorem 2.2], if V has compact support in Ω then the shape derivative vanishes. Assume $V \in \mathcal{C}_c^1(\Omega \setminus \Gamma_h, \mathbb{R}^2)$ and denote $U := \operatorname{supp} V \subset \Omega \setminus \Gamma_h$, then u and p are clearly harmonic on U since σ is constant on U . In view of (19) and the regularity of f_{Ω} , this yields $\mathbf{S}_1 \in L^1(U)$ and $\operatorname{div}(\mathbf{S}_1) \in L^1(U)$. Thus, we can write the tensor relation $\operatorname{div}(\mathbf{S}_1^T V) = \mathbf{S}_1 : DV + V \cdot \operatorname{div}(\mathbf{S}_1)$. For such V we also have $\mathbf{S}_0^s(V) = 0$, so we obtain

$$\begin{aligned} dJ(\Omega)(V) &= \mathbf{S}_0^s(V) + \int_{\mathcal{D}} \mathbf{S}_1 : DV + \mathbf{S}_0^r \cdot V \\ &= \int_U \operatorname{div}(\mathbf{S}_1^T V) + V \cdot (\mathbf{S}_0^r - \operatorname{div} \mathbf{S}_1) = 0 \quad \text{for all } V \in \mathcal{C}_c^1(\Omega \setminus \Gamma_h, \mathbb{R}^2). \end{aligned} \quad (42)$$

Since $\operatorname{supp} V = U \subset \Omega \setminus \Gamma_h$, we can extend $\mathbf{S}_1^T V$ and $V \cdot (\mathbf{S}_0^r - \operatorname{div} \mathbf{S}_1)$ by zero on \mathcal{B} , where \mathcal{B} is a sufficiently large open ball which contains U . We keep the same notation for the extensions for simplicity. Since the extension satisfies $\mathbf{S}_1^T V \in W^{1,1}(\mathcal{B}, \mathbb{R}^2)$, using the divergence theorem (for instance [23, Section 4.3, Theorem 1]) in \mathcal{B} we get

$$\begin{aligned} \int_U \operatorname{div}(\mathbf{S}_1^T V) + V \cdot (\mathbf{S}_0^r - \operatorname{div} \mathbf{S}_1) &= \int_{\mathcal{B}} \operatorname{div}(\mathbf{S}_1^T V) + V \cdot (\mathbf{S}_0^r - \operatorname{div} \mathbf{S}_1) \\ &= \int_{\partial\mathcal{B}} (\mathbf{S}_1^T V) \cdot n + \int_{\mathcal{B}} V \cdot (\mathbf{S}_0^r - \operatorname{div} \mathbf{S}_1) \\ &= \int_{\Omega} V \cdot (\mathbf{S}_0^r - \operatorname{div} \mathbf{S}_1) = 0, \quad \text{for all } V \in \mathcal{C}_c^1(\Omega \setminus \Gamma_h, \mathbb{R}^2), \end{aligned}$$

which proves (37). Then, we can prove (38) in a similar way by taking a vector $V \in \mathcal{C}_c^1((\mathcal{D} \setminus \bar{\Omega}) \setminus \Gamma_h, \mathbb{R}^2)$.

Now let us assume that $V \in \mathcal{C}_c^1(\mathcal{D} \setminus \Gamma_h, \mathbb{R}^2)$ and denote $U_2 := \operatorname{supp} V \subset \mathcal{D} \setminus \Gamma_h$. By standard elliptic regularity, we have $u \in H^1(U_2)$ and $p \in H^1(U_2)$. If we assume $\mathbf{S}_1^+ \in W^{1,1}(\Omega, \mathbb{R}^{2 \times 2})$ and

$\mathbf{S}_1^- \in W^{1,1}(\mathcal{D} \setminus \bar{\Omega}, \mathbb{R}^{2 \times 2})$, taking $V \in \mathcal{C}_c^1(\mathcal{D} \setminus \Gamma_h, \mathbb{R}^2)$ and using (37)-(38) we obtain

$$\begin{aligned} dJ(\Omega)(V) &= \mathbf{S}_0(V) + \int_{\mathcal{D}} \mathbf{S}_1 : DV + \mathbf{S}_0^r \cdot V \\ &= \int_{\Omega} \mathbf{S}_1 : DV + \mathbf{S}_0^r \cdot V + \int_{\mathcal{D} \setminus \bar{\Omega}} \mathbf{S}_1 : DV + \mathbf{S}_0^r \cdot V \\ &= \int_{\Omega} \operatorname{div}(\mathbf{S}_1^T V) + V \cdot (\mathbf{S}_0^r - \operatorname{div} \mathbf{S}_1) + \int_{\mathcal{D} \setminus \bar{\Omega}} \operatorname{div}(\mathbf{S}_1^T V) + V \cdot (\mathbf{S}_0^r - \operatorname{div} \mathbf{S}_1) \\ &= \int_{\Omega} \operatorname{div}(\mathbf{S}_1^T V) + \int_{\mathcal{D} \setminus \bar{\Omega}} \operatorname{div}(\mathbf{S}_1^T V), \end{aligned}$$

which yields (39). If in addition Ω is Lipschitz, applying the divergence theorem to (39) we get (40).

In view of (40), we have that $dJ(\Omega)$ is continuous for the $\mathcal{C}^0(\mathcal{D}, \mathbb{R}^d)$ -topology. Thus, if Ω is of class \mathcal{C}^1 , we can apply Theorem 3.3 with $k = 0$. With Ω of class \mathcal{C}^1 , we also have $n \in \mathcal{C}^0(\partial\Omega, \mathbb{R}^2)$ and $(V|_{\partial\Omega} \cdot n)n \in \mathcal{C}^0(\partial\Omega, \mathbb{R}^2)$. Let $\hat{V} \in \mathcal{C}_c^0(\mathcal{D} \setminus \Gamma_h, \mathbb{R}^2)$ be an extension of $(V|_{\partial\Omega} \cdot n)n$, then using Theorem 3.3 we obtain

$$\begin{aligned} dJ(\Omega)(V) &= l(V|_{\partial\Omega} \cdot n) = l(\hat{V}|_{\partial\Omega} \cdot n) = dJ(\Omega)(\hat{V}) \\ &= \int_{\partial\Omega} ((\mathbf{S}_1^+ - \mathbf{S}_1^-)n) \cdot \hat{V} = \int_{\partial\Omega} (\llbracket \mathbf{S}_1 \rrbracket n) \cdot ((V \cdot n)n) = \int_{\partial\Omega} (\llbracket \mathbf{S}_1 \rrbracket n \cdot n) V \cdot n, \end{aligned}$$

which yields expression (41). \square

Remark 3.5. Proposition 3.4 is in fact valid for any shape functional whose distributed shape derivative can be written using a tensor expression of the type (18), and which satisfies the appropriate regularity assumptions. Note that in general, one should not expect that the assumption $\mathbf{S}_1^+ \in W^{1,1}(\Omega, \mathbb{R}^{2 \times 2})$ and $\mathbf{S}_1^- \in W^{1,1}(\mathcal{D} \setminus \bar{\Omega}, \mathbb{R}^{2 \times 2})$ in Proposition 3.4 can be satisfied for any Lipschitz set Ω . For instance in the case of the Dirichlet Laplacian, one can actually build pathological Lipschitz domains for which \mathbf{S}_1 does not have such regularity; see [17, Corollary 3.2]. However, these regularity assumptions for $\mathbf{S}_1^+, \mathbf{S}_1^-$ can be fulfilled for polygonal domains, as shown in Corollary 3.6.

Corollary 3.6. *Suppose that $\Gamma_h \cap \partial\Omega = \emptyset$, $f_0 \in \mathcal{C}^\infty(\mathcal{D})$, $\Omega \in \mathbb{P}(\mathcal{D})$ and $V \in \mathcal{C}_c^1(\mathcal{D} \setminus \Gamma_h, \mathbb{R}^2)$. If Ω is Lipschitz polygonal or if Ω is of class \mathcal{C}^1 , then we have*

$$dJ(\Omega)(V) = \int_{\partial\Omega} (\llbracket \sigma \partial_n u \partial_n p \rrbracket + \llbracket \sigma \rrbracket \nabla_{\partial\Omega} u \cdot \nabla_{\partial\Omega} p - \llbracket f_\Omega \rrbracket p) V \cdot n, \quad (43)$$

where $\nabla_{\partial\Omega}$ denotes the tangential gradient on $\partial\Omega$.

Proof. In the case where Ω is of class \mathcal{C}^1 , a quick calculation using (41) and (19) yields (43).

In the case where Ω is polygonal, we can proceed in the following way. Let $\hat{\mathcal{D}}$ be a smooth open set such that $\bar{\Omega} \subset \hat{\mathcal{D}} \subset \mathcal{D}$ and the boundaries of Ω and $\hat{\mathcal{D}}$ are at a positive distance. Since $f_0 \in \mathcal{C}^\infty(\mathcal{D})$, using elliptic regularity we get that u and p are \mathcal{C}^∞ on $\partial\hat{\mathcal{D}}$. Thus, $u|_{\hat{\mathcal{D}}}$ and $p|_{\hat{\mathcal{D}}}$ are also solutions of transmission problems defined in $\hat{\mathcal{D}}$ with smooth inhomogeneous Dirichlet conditions on $\partial\hat{\mathcal{D}}$, and consequently we are in the framework considered in [56]. Denote L the number of vertices of the polygon Ω . We apply [56, Theorem 7.3] in the case $k = 0$, $m = 1$ and for the regularity $W^{2,4/3}$. This yields the decomposition $u|_{\hat{\mathcal{D}}} = u_0 + \sum_{\ell \in L} S_\ell$ with $u_0^+ \in W^{2,4/3}(\Omega)$, $u_0^- \in W^{2,4/3}(\hat{\mathcal{D}} \setminus \bar{\Omega})$ and S_ℓ are singular functions with support in the neighbourhood of the vertices of Ω . Here $S_\ell(r_\ell, \theta_\ell)$ are of the type $r_\ell^{\lambda_\ell} v(r_\ell, \theta_\ell)$, where (r_ℓ, θ_ℓ) are local polar coordinates at the vertex ℓ and $v(\theta_\ell)$ is a linear combination of $\sin(\lambda_\ell \theta_\ell)$ and $\cos(\lambda_\ell \theta_\ell)$. It is shown in [18, Theorem 8.1(ii)] that $\lambda_\ell > 1/2$ for all $\ell = 1, \dots, L$. Thus, we also obtain $\sum_{\ell \in L} S_\ell^+ \in W^{2,4/3}(\Omega)$ and $\sum_{\ell \in L} S_\ell^- \in W^{2,4/3}(\hat{\mathcal{D}} \setminus \bar{\Omega})$.

Proceeding in a similar way for p and gathering the results, we obtain the regularity $u^+, p^+ \in W^{2,4/3}(\Omega)$ and $u^-, p^- \in W^{2,4/3}(\hat{\mathcal{D}} \setminus \bar{\Omega})$. Then we have $\nabla(\nabla u \cdot \nabla p) = D^2 u p + D^2 p u$ and using $(D^2 u)^+, (D^2 p)^+ \in L^{4/3}(\Omega)$ and $(\nabla u)^+, (\nabla p)^+ \in W^{1,4/3}(\Omega) \subset L^4(\Omega)$ and the same regularity on $\hat{\mathcal{D}} \setminus \bar{\Omega}$, we obtain $\mathbf{S}_1^+ \in W^{1,1}(\Omega, \mathbb{R}^{2 \times 2})$ and $\mathbf{S}_1^- \in W^{1,1}(\hat{\mathcal{D}} \setminus \bar{\Omega}, \mathbb{R}^{2 \times 2})$.

Then, using the fact that $V \in \mathcal{C}_c^1(\mathcal{D} \setminus \Gamma_h, \mathbb{R}^2)$ we obtain in view of (40) of Proposition 3.4

$$dJ(\Omega)(V) = \int_{\partial\Omega} [\![\sigma \partial_n u]\!] \nabla_{\partial\Omega} u \cdot V + [\![\sigma \partial_n p]\!] \nabla_{\partial\Omega} p \cdot V + ([\![\sigma \partial_n u \partial_n p]\!] + [\![\sigma]\!] \nabla_{\partial\Omega} u \cdot \nabla_{\partial\Omega} p - [\![f_\Omega]\!] p) V \cdot n.$$

Finally, using the fact that $[\![\sigma \partial_n u]\!] = 0$ and $[\![\sigma \partial_n p]\!] = 0$ we obtain (43). \square

Remark 3.7. Expressions similar to (43) are known when Ω is at least \mathcal{C}^1 , see [54] and [2]. It is remarkable that one obtains the same expression (43) when Ω is only Lipschitz polygonal. Also, note that (43) is similar to the formula obtained in [9] for a polygonal inclusion in EIT, which was obtained in the framework of the perturbation of identity method. In [9], an estimate of the singularity of the gradient in the neighbourhood of the vertices of the polygonal inclusion was used to obtain the boundary expression. Here, we have used higher regularity of u and p in the subdomains Ω and $\widehat{\mathcal{D}} \setminus \overline{\Omega}$ to obtain (43). The key idea of these two approaches is to control the singularity of the gradients of u and p near the vertices of the polygonal inclusion.

4 Numerical experiments

We use the software package FEniCS for the implementation; see [4, 53, 55]. For the numerical tests the conductivity values are set to $\sigma_0 = 1$ and $\sigma_1 = 10$. We choose $f_\Omega \equiv 0$, $\mathcal{D} = (0, 1) \times (0, 1)$ and

$$\Gamma = \partial\mathcal{D} \setminus ([0.4, 0.6] \times \{0\} \cup [0.4, 0.6] \times \{1\}).$$

The domain \mathcal{D} is meshed using a regular grid of 128×128 elements. For the measurement points we choose $\Gamma_h = \{x_k\}_{k=1}^K \subset \Gamma$. Recall that no measurements are performed on $\Gamma_0 = \partial\mathcal{D} \setminus \Gamma$ and that u satisfies Dirichlet boundary condition on Γ_0 .

Synthetic measurements $\{h_i(x_k)\}_{k=1}^K$ are obtained by taking the trace on Γ of the solution of (7) using the ground truth domain Ω^* , $f_{\Omega^*} \equiv 0$ and currents g_i , $i = 1, \dots, I$. To simulate noisy EIT data, each measurement h_i is corrupted by adding a normal Gaussian noise with mean zero and standard deviation $\delta * \|h_i\|_\infty$, where δ is a parameter. The noise level is then computed as

$$noise = \frac{\sum_{i=1}^I (\sum_{k=1}^K |h_i(x_k) - \tilde{h}_i(x_k)|^2)^{1/2}}{\sum_{i=1}^I (\sum_{k=1}^K |h_i(x_k)|^2)^{1/2}}, \quad (44)$$

where $h_i(x_k)$ and $\tilde{h}_i(x_k)$ are respectively the noiseless and noisy point measurements at x_k corresponding to the current g_i .

In the numerical tests, we use two different sets of fluxes, i.e. $I \in \{3, 7\}$, to obtain measurements. Denote Γ_{upper} , Γ_{lower} , Γ_{left} and Γ_{right} the four sides of the square Ω . When $I = 3$ we take

$$\begin{aligned} g_1 &= 1 \text{ on } \Gamma_{\text{left}} \cup \Gamma_{\text{right}} \text{ and } g_1 = -1 \text{ on } \Gamma_{\text{upper}} \cup \Gamma_{\text{lower}}, \\ g_2 &= 1 \text{ on } \Gamma_{\text{left}} \cup \Gamma_{\text{upper}} \text{ and } g_2 = -1 \text{ on } \Gamma_{\text{right}} \cup \Gamma_{\text{lower}}, \\ g_3 &= 1 \text{ on } \Gamma_{\text{left}} \cup \Gamma_{\text{lower}} \text{ and } g_3 = -1 \text{ on } \Gamma_{\text{right}} \cup \Gamma_{\text{upper}}. \end{aligned}$$

When $I = 7$ we take in addition a smooth approximation of the following piecewise constant function:

$$g_4 = 1 \text{ on } \Gamma_{\text{left}} \cap \{x_2 > 0.5\}, \quad g_4 = -1 \text{ on } \Gamma_{\text{left}} \cap \{x_2 \leq 0.5\} \text{ and } g_4 = 0 \text{ otherwise,}$$

and g_5, g_6, g_7 are defined in a similar way on Γ_{right} , Γ_{upper} , Γ_{lower} , respectively.

For the numerics we use the cost functional given by (10):

$$J(\Omega) = \frac{1}{2} \sum_{i=1}^I \mu_i \sum_{k=1}^K (u_i(x_k) - h(x_k))^2, \quad (45)$$

where u_i is the potential associated with the current g_i . The weights μ_i associated with the current g_i are chosen as the inverse of $\sum_{k=1}^K (u_i(x_k) - h(x_k))^2$ computed at the initial guess. In this way, each term in the sum over I is equal to 1 at the first iteration, and the initial value of $J(\Omega)$ is equal to $I/2$.

To get a relatively smooth descent direction we solve the following partial differential equation: find $V \in H_0^1(\mathcal{D})^2$ such that

$$\int_{\mathcal{D}} \alpha_1 DV : D\xi + \alpha_2 V \cdot \xi = -dJ(\Omega)(\xi) \text{ for all } \xi \in H_0^1(\mathcal{D})^2.$$

For the numerical tests, we chose $\alpha_1 = 0.3$ and $\alpha_2 = 0.7$. To simplify the implementation, we use Dirichlet conditions on $\partial\mathcal{D}$ instead of the compact support condition $V \in \mathcal{C}_c^1(\mathcal{D} \setminus \Gamma_h, \mathbb{R}^2)$ (see Section 2.2). Considering that $f_\Omega \equiv 0$ in \mathcal{D} , $V = 0$ on $\partial\mathcal{D}$ and that the points $\{x_k\}_{k=1}^K$ belong to Γ , in view of Theorem 3.2 we get $\mathbf{S}_0^s(V) = 0$ which leads to the following equation for V :

$$\int_{\mathcal{D}} \alpha_1 DV : D\xi + \alpha_2 V \cdot \xi = - \int_{\mathcal{D}} -2\sigma_\Omega(\nabla u \odot \nabla p) : D\xi + (\sigma_\Omega \nabla u \cdot \nabla p) \mathbb{I} : D\xi \quad \text{for all } \xi \in H_0^1(\mathcal{D})^2.$$

The relative reconstruction error $E(\Omega^r)$ is defined as

$$E(\Omega^r) := \frac{\int_{\mathcal{D}} |\chi_{\Omega^*} - \chi_{\Omega^r}|}{\int_{\mathcal{D}} \chi_{\Omega^*}},$$

where Ω^r is the set obtained in the last iteration of the minimization algorithm. We use $E(\Omega^r)$ as a measure of the quality of the reconstructions.

We present three numerical experiments. In the first experiment, the ground truth consists of two ellipses and we use $I = 3$ currents; see Figure 2. In the second experiment, the ground truth is a concave shape with one connected component and we use $I = 3$ currents; see Figure 4. In the third experiment, the ground truth consists of two ellipses and one ball and we use $I = 7$ currents; see Figure 6. For each experiment, we study the influence of the point measurements patterns by comparing the reconstructions obtained using three different sets $\Gamma_h = \{x_k\}_{k=1}^K$ with $K \in \{16, 34, 70\}$. The point measurements patterns and the corresponding reconstructions are presented in Figures 3, 5 and 7, for the respective experiments. We observe, as expected, that the reconstructions improve as K becomes larger. However, one obtains reasonable reconstructions in the case of the concave shape with $I = 3$ currents and in the case of the two ellipses and ball with $I = 7$ currents, even for $K = 16$ points and in the presence of noise; see Figures 5 and 7. In the case of two ellipses, the deterioration of the reconstruction for $K = 16$ points is much stronger compared to the case $K = 70$. This indicates that the number of current $I = 3$ is too low to reconstruct two ellipses with only $K = 16$ points. We conclude from these results that the amount of applied currents is more critical than the number of point measurements to obtain a good reconstruction.

For each experiment, we also study how the noise level affects the reconstruction depending on the amount of point measurements. The results are gathered in Tables 1, 2 and 3, where the rows correspond to three different levels of noise, and the columns to three different numbers of points $K \in \{16, 34, 70\}$. In the case of two ellipses (Table 1), the reconstruction using $K = 70$ is very robust with respect to noise, whereas it deteriorates considerably using $K = 16$. In the cases of the concave shape (Table 2) and of the two ellipses and ball (Table 3), the degradations of the reconstructions when the noise becomes larger are of a similar order in terms of reconstruction error, independently of the value of K . These results indicate that a larger number of points K may improve the robustness of the reconstruction with respect to noise mainly when the number I of currents is low compared to the complexity of the ground truth.

Acknowledgements. Yuri Flores Albuquerque and Antoine Laurain gratefully acknowledge support of the RCGI - Research Centre for Gas Innovation, hosted by the University of São Paulo (USP) and sponsored by FAPESP - São Paulo Research Foundation (2014/50279-4) and Shell Brasil. This research was carried out in association with the ongoing R&D project registered as ANP 20714-2 - Desenvolvimento de técnicas numéricas e software para problemas de inversão com aplicações em processamento sísmico (USP / Shell Brasil / ANP), sponsored by Shell Brasil under the ANP R&D levy as “Compromisso de Investimentos com Pesquisa e Desenvolvimento”. Antoine Laurain gratefully acknowledges the support of FAPESP, process: 2016/24776-6 “Otimização de forma e problemas de fronteira livre”, and of the Brazilian National Council for Scientific and Technological Development (Conselho Nacional de Desenvolvimento Científico e Tecnológico - CNPq) through the process: 408175/2018-4 “Otimização de forma

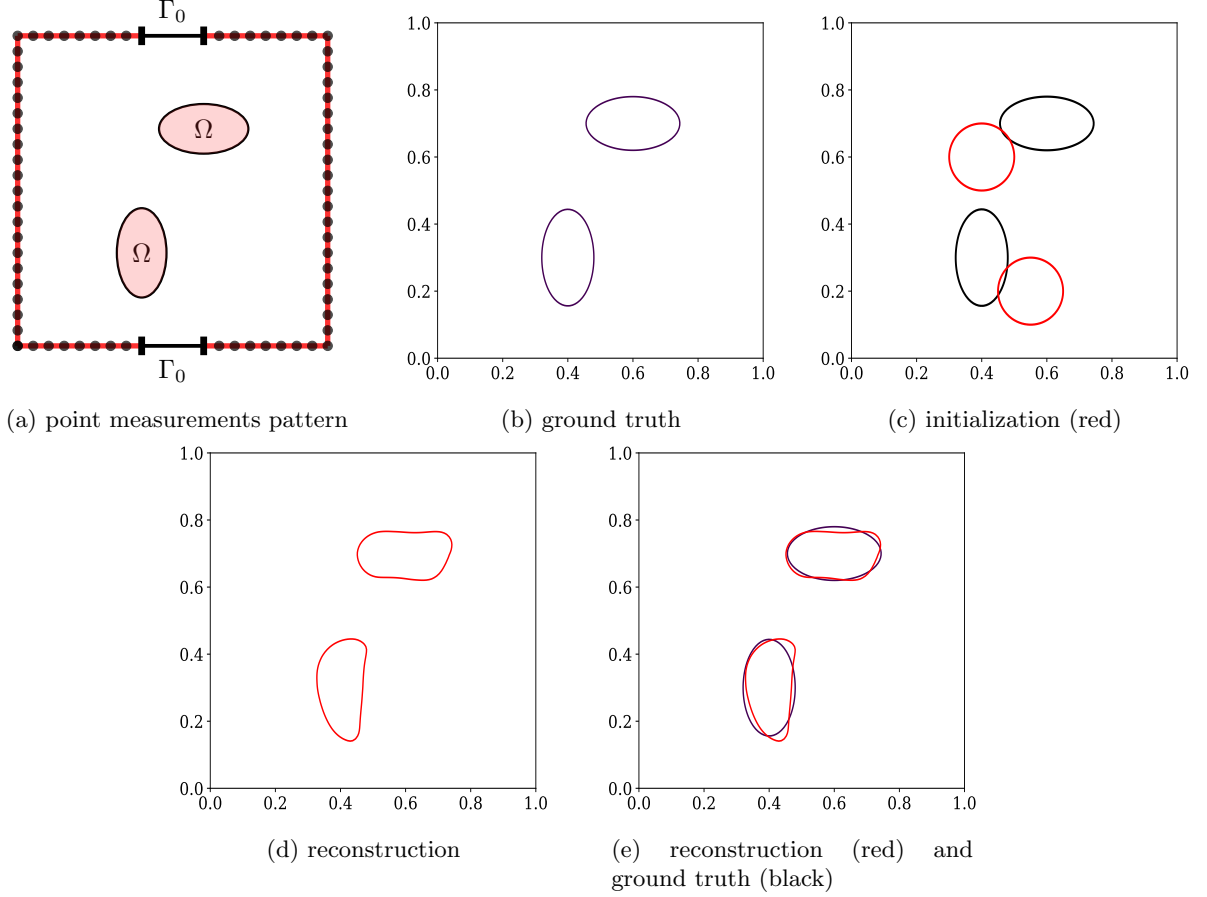


Figure 2: Reconstruction of two ellipses using $I = 3$ currents and $K = 70$ point measurements with 1.13% noise.

não suave e controle de problemas de fronteira livre”, and through the program “Bolsa de Produtividade em Pesquisa - PQ 2018”, process: 304258/2018-0.

5 Appendix 1: averaged adjoint method

Let $t_0 > 0$ be given and $E = E(\mathcal{D}), F = F(\mathcal{D})$ be two Banach spaces, and consider a parameterization $\Omega_t = T_t(\Omega)$ for $t \in [0, t_0]$ such that $T_t(\mathcal{D}) = \mathcal{D}$, i.e. which leaves \mathcal{D} globally invariant. Our goal is to differentiate shape functions of the type $J(\Omega_t)$ which can be written using a Lagrangian as $J(\Omega_t) = \mathcal{L}(\Omega_t, u^t, \hat{\psi})$, where $u^t \in E(\mathcal{D})$ and $\hat{\psi} \in F(\mathcal{D})$. The main appeal of the Lagrangian is that we actually only need to compute the partial derivative with respect to t of $\mathcal{L}(\Omega_t, \hat{\varphi}, \hat{\psi})$ to compute the derivative of $J(\Omega_t)$, indeed this is the main result of Theorem 5.3.

In order to differentiate $\mathcal{L}(\Omega_t, \hat{\varphi}, \hat{\psi})$, the change of coordinates $x \mapsto T_t(x)$ is used in the integrals. In the process appear the pullbacks $\hat{\varphi} \circ T_t \in E(\mathcal{D})$ and $\hat{\psi} \circ T_t \in F(\mathcal{D})$ which depend on t . The usual procedure in shape optimization to compensate this effect is to use a reparameterization $\mathcal{L}(\Omega_t, \Psi_t(\varphi), \Psi_t(\psi))$ instead of $\mathcal{L}(\Omega_t, \hat{\varphi}, \hat{\psi})$, where Ψ_t is an appropriate bijection of $E(\mathcal{D})$ and $F(\mathcal{D})$, and $\varphi \in E(\mathcal{D}), \psi \in F(\mathcal{D})$. Now the change of variable in the integrals yields functions φ and ψ in the integrands, which are independent of t . In this paper we take $E(\mathcal{D}) = W_{\Gamma, p}^1(\mathcal{D}), F(\mathcal{D}) = W_{\Gamma, p'}^1(\mathcal{D})$, and $\Psi_t(\psi) = \psi \circ T_t^{-1}$ is then a bijection of $E(\mathcal{D})$ and $F(\mathcal{D})$; see [64, Theorem 2.2.2, p.52].

Thus we consider the so-called *shape-Lagrangian* $G : [0, t_0] \times E \times F \rightarrow \mathbb{R}$ with

$$G(t, \varphi, \psi) := \mathcal{L}(\Omega_t, \varphi \circ T_t^{-1}, \psi \circ T_t^{-1}).$$

The main result of this section, Theorem 5.3, shows that in order to obtain the shape derivative of \mathcal{L} , it

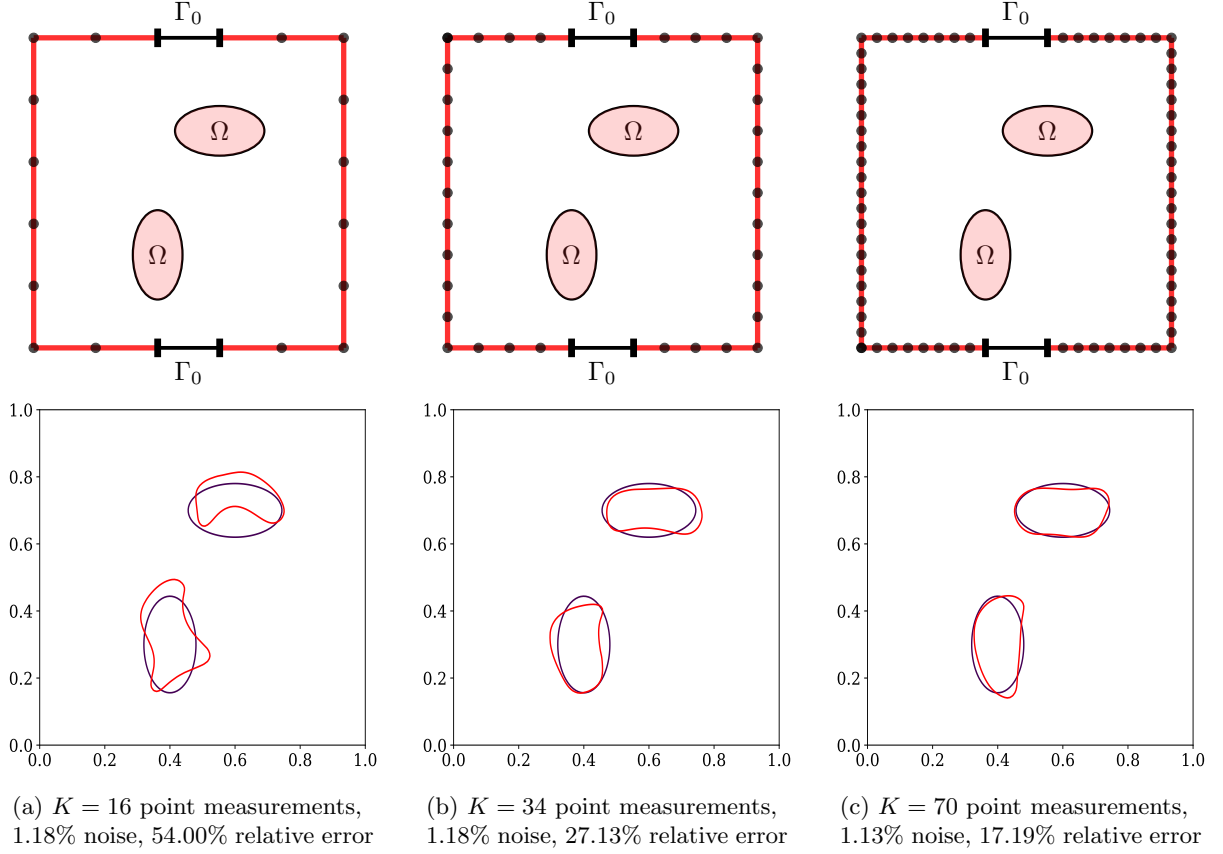


Figure 3: Reconstruction of two ellipses using $I = 3$ currents and three different sets of point measurements shown in the first row.

is enough to compute the partial derivative with respect to t of G while assigning the values $\varphi = u$ and $\psi = p$, where u is the state and p is the adjoint state. The main ingredient is the introduction of the averaged adjoint equation described below.

Let us assume that for each $t \in [0, t_0]$ the equation

$$d_\psi G(t, u^t, 0; \hat{\psi}) = 0 \quad \text{for all } \hat{\psi} \in F. \quad (46)$$

admits a unique solution $u^t \in E$. Further, we make the following assumptions for G .

Assumption 5.1. For every $(t, \psi) \in [0, t_0] \times F$

- (i) $[0, 1] \ni s \mapsto G(t, su^t + (1-s)u^0, \psi)$ is absolutely continuous.
- (ii) $[0, 1] \ni s \mapsto d_\varphi G(t, su^t + (1-s)u^0, \psi; \hat{\varphi})$ belongs to $L^1(0, 1)$ for all $\hat{\varphi} \in E$.

When Assumption 5.1 is satisfied, for $t \in [0, t_0]$ we introduce the *averaged adjoint equation* associated with u^t and u^0 : find $p^t \in F$ such that

$$\int_0^1 d_\varphi G(t, su^t + (1-s)u^0, p^t; \hat{\varphi}) ds = 0 \quad \text{for all } \hat{\varphi} \in E. \quad (47)$$

In view of Assumption 5.1 we have

$$G(t, u^t, p^t) - G(t, u^0, p^t) = \int_0^1 d_\varphi G(t, su^t + (1-s)u^0, p^t; u^t - u^0) ds = 0 \quad \text{for all } t \in [0, t_0]. \quad (48)$$

We can now state the main result of this section.

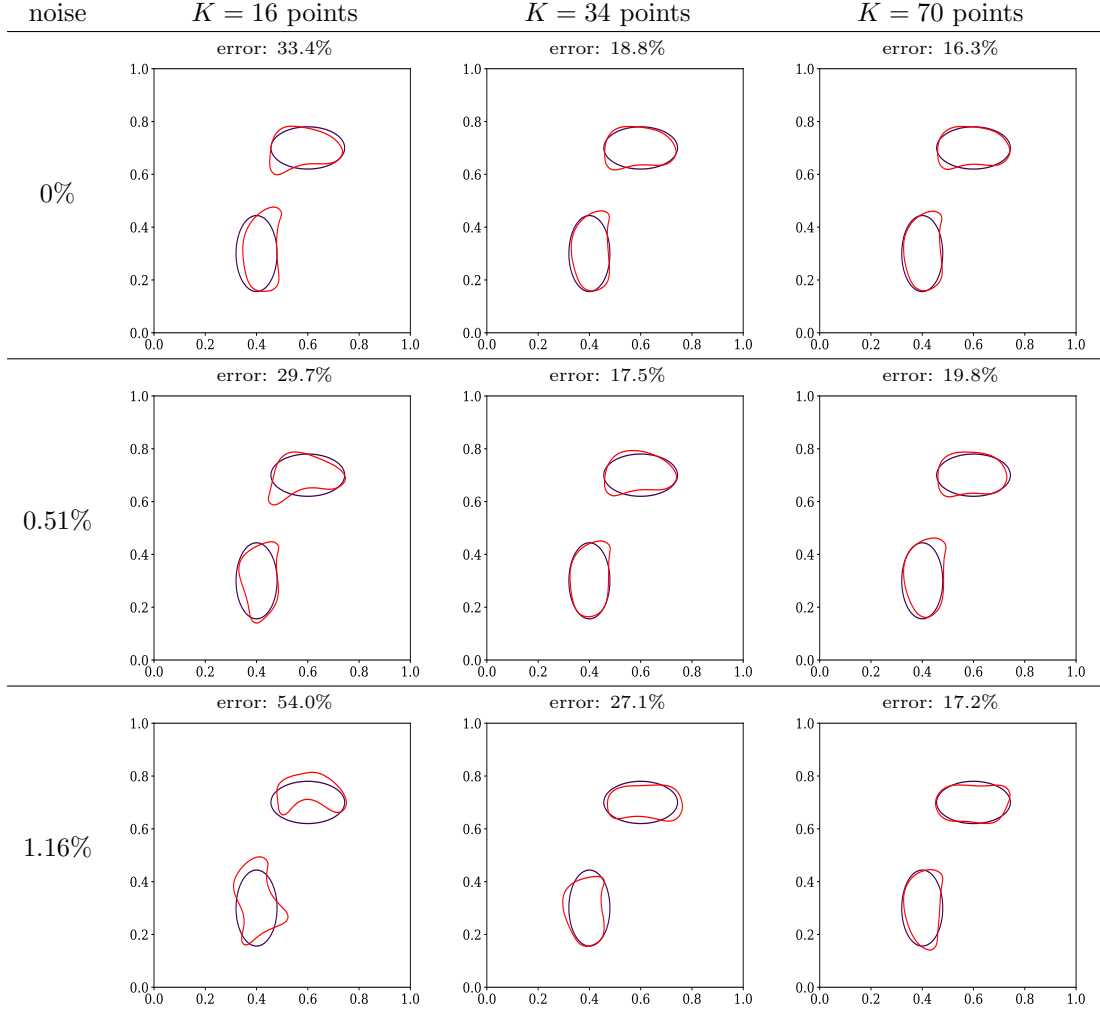


Table 1: Influence of noise and number of point measurements on the reconstruction of two ellipses using $I = 3$ currents (the noise value is the average over the noise values for the three levels of point measurements).

Assumption 5.2. *We assume that*

$$\lim_{t \searrow 0} \frac{G(t, u^0, p^t) - G(0, u^0, p^t)}{t} = \partial_t G(0, u^0, p^0).$$

Theorem 5.3. *Let Assumption 5.1 and Assumption 5.2 be satisfied and assume there exists a unique solution p^t of the averaged adjoint equation (47). Then for all $\psi \in F$ we obtain*

$$\frac{d}{dt} b(t, u^t)|_{t=0} = \frac{d}{dt} (G(t, u^t, \psi))|_{t=0} = \partial_t G(0, u^0, p^0). \quad (49)$$

6 Appendix 2: proof of Theorem 2.4

For the convenience of the reader we write here the proof of Theorem 2.4, which is essentially the same as the proof of [31, Theorem 1]. We recall from [30] that if $\mathcal{D} \cup \Gamma$ is regular in the sense of Gröger, then the mapping $\mathcal{P} : W_{\Gamma, q}^1(\mathcal{D}) \rightarrow (W_{\Gamma, q'}^1(\mathcal{D}))^*$ defined by

$$\langle \mathcal{P}v, w \rangle := \int_{\mathcal{D}} \nabla v \cdot \nabla w + vw$$

is onto and hence the inverse $\mathcal{P}^{-1} : (W_{\Gamma, q'}^1(\mathcal{D}))^* \rightarrow W_{\Gamma, q}^1(\mathcal{D})$ is well-defined.

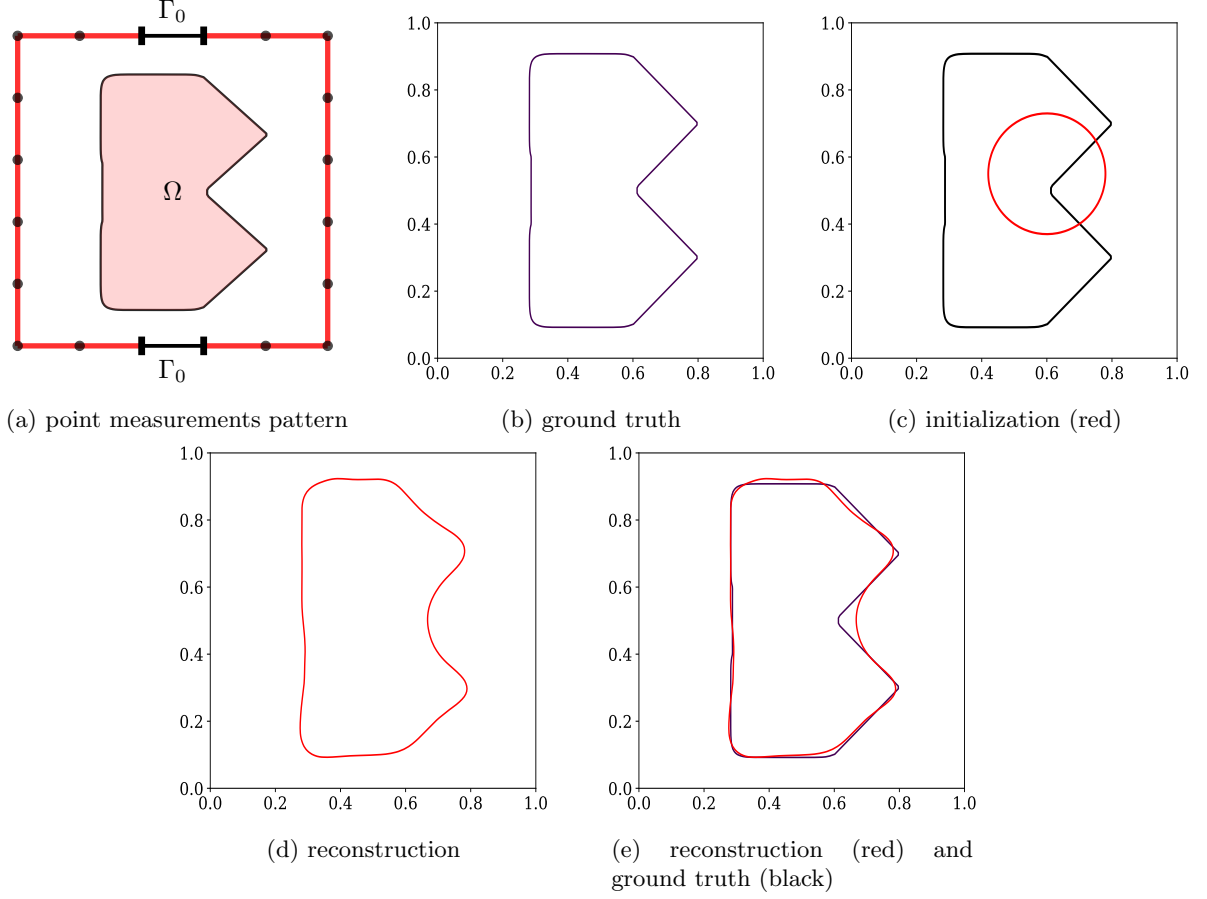


Figure 4: Reconstruction of a concave shape using $I = 3$ currents and $K = 34$ point measurements with 0.55% noise.

Proof of Theorem 2.4. Let $f \in (W_{\Gamma,q'}^1(\mathcal{D}))^*$ be given. As in [31, Theorem 1] we define for $s > 0$ the mapping

$$Q_f : W_{\Gamma,q}^1(\mathcal{D}) \rightarrow W_{\Gamma,q}^1(\mathcal{D}),$$

$$u \mapsto \mathcal{P}^{-1}(D^*BDu + tf),$$

where $D : W_{\Gamma,2}^1(\mathcal{D}) \rightarrow L^2(\mathcal{D}, \mathbb{R}^3)$ is defined by $u \mapsto (u, \nabla u)$, $D^* : L^2(\mathcal{D}, \mathbb{R}^3)^* \rightarrow (W_{\Gamma,2}^1(\mathcal{D}))^*$ is the adjoint of D and $By := y - s\hat{\mathbb{A}}y$ for $y = (y_0, y_1, y_2) \in L^2(\mathcal{D}, \mathbb{R}^3)$ and $\hat{\mathbb{A}}y := (0, \mathbb{A}(y_1, y_2)^\top)$. We observe that $D^*BDu = D^*Du - sD^*(0, \mathbb{A}\nabla u)$ and $D^*D = \mathcal{P}$, which yields

$$Q_fu = u - s\mathcal{P}^{-1}(D^*(0, \mathbb{A}\nabla u) - f).$$

If Q_f has a fixed point in $W_{\Gamma,q}^1(\mathcal{D})$, then we obtain $D^*(0, \mathbb{A}\nabla u) = f$ in $(W_{\Gamma,q'}^1(\mathcal{D}))^*$ which is equivalent to $\mathcal{A}_qu = f$ in $(W_{\Gamma,q'}^1(\mathcal{D}))^*$. The proper choice of s allows to show that Q_f is a contraction and the result follows from Banach's fixed point theorem. Note that $\|D\|_{L^2} = \|D^*\|_{L^2} = 1$. Then for all $v, w \in W_{\Gamma,q}^1(\mathcal{D})$ we have

$$\|Q_f v - Q_f w\|_{W_q^1} \leq \|\mathcal{P}^{-1}\|_{L(W_{\Gamma,q}^{-1}, W_{\Gamma,q}^1)} \|D^*\|_{L^2} \|BD(v - w)\|_{L^q}. \quad (50)$$

Now, using assumptions (1) yields, for all $s > 0$,

$$|By(x)|^2 = |y(x)|^2 - 2s\hat{\mathbb{A}}(x)y(x) \cdot y(x) + s^2|\hat{\mathbb{A}}(x)y(x)|^2$$

$$\leq |y(x)|^2 - 2ms|y(x)|^2 + s^2M^2|y(x)|^2. \quad (51)$$

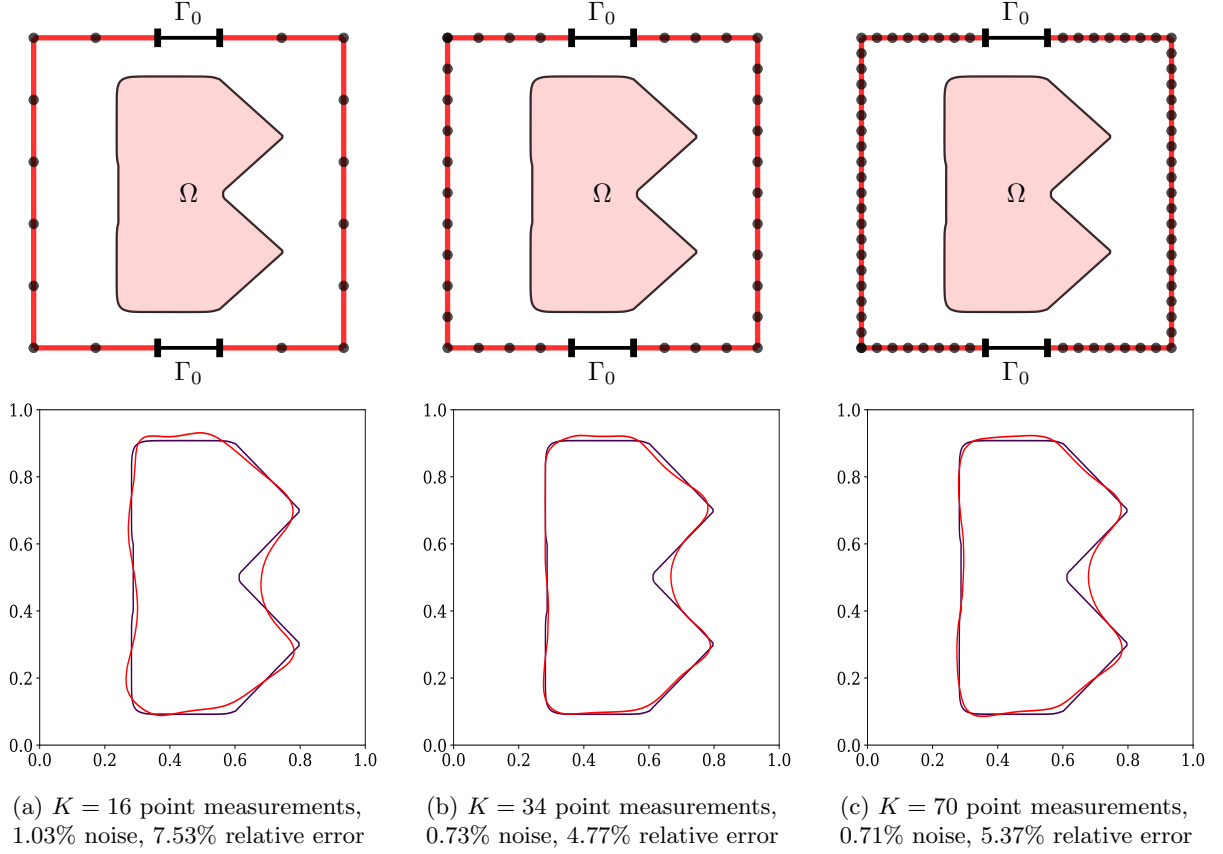


Figure 5: Reconstruction of a concave shape using $I = 3$ currents and three different sets of point measurements shown in the first row.

Hence, choosing $s = m/M^2$ yields $|By(x)| \leq k|y(x)|$ with $k := (1 - m^2/M^2)^{1/2}$ and thus

$$\|BD(u - v)\|_{L^q} \stackrel{(51)}{\leq} k\|D(u - v)\|_{L^q}. \quad (52)$$

Combining (50), (52), $M_q = \|\mathcal{P}^{-1}\|_{L(W_{\Gamma,q}^{-1}, W_{\Gamma,q}^1)}$ and $\|D\|_{L^2} = 1$ yields

$$\|Q_f u - Q_g v\|_{W_q^1} \leq kM_q \|u - v\|_{W_q^1}.$$

Since we have assumed that $kM_q < 1$, it follows that Q_f is a contraction.

Let u and v be the fixed points of Q_f, Q_g , respectively. Then we have

$$\begin{aligned} \|u - v\|_{W_q^1} &= \|Q_f u - Q_g v\|_{W_q^1} \leq kM_q \|u - v\|_{W_q^1} + \|Q_f v - Q_g v\|_{W_q^1} \\ &\leq kM_q \|u - v\|_{W_q^1} + t\|\mathcal{P}^{-1}\|_{L(W_{\Gamma,q}^{-1}, W_{\Gamma,q}^1)} \|f - g\|_{W_{\Gamma,q}^{-1}}. \end{aligned}$$

Using $M_q = \|\mathcal{P}^{-1}\|_{L(W_{\Gamma,q}^{-1}, W_{\Gamma,q}^1)}$ we obtain

$$(1 - kM_q)\|u - v\|_{W_q^1} \leq tM_q \|f - g\|_{W_{\Gamma,q}^{-1}}.$$

which proves (3). By Lemma 2.3 the hypothesis $M_q k < 1$ of Theorem 2.4 is satisfied if $q > 2$ is sufficiently close to 2. \square

References

- [1] R. A. Adams and J. J. F. Fournier. *Sobolev spaces*, volume 140 of *Pure and Applied Mathematics (Amsterdam)*. Elsevier/Academic Press, Amsterdam, second edition, 2003.

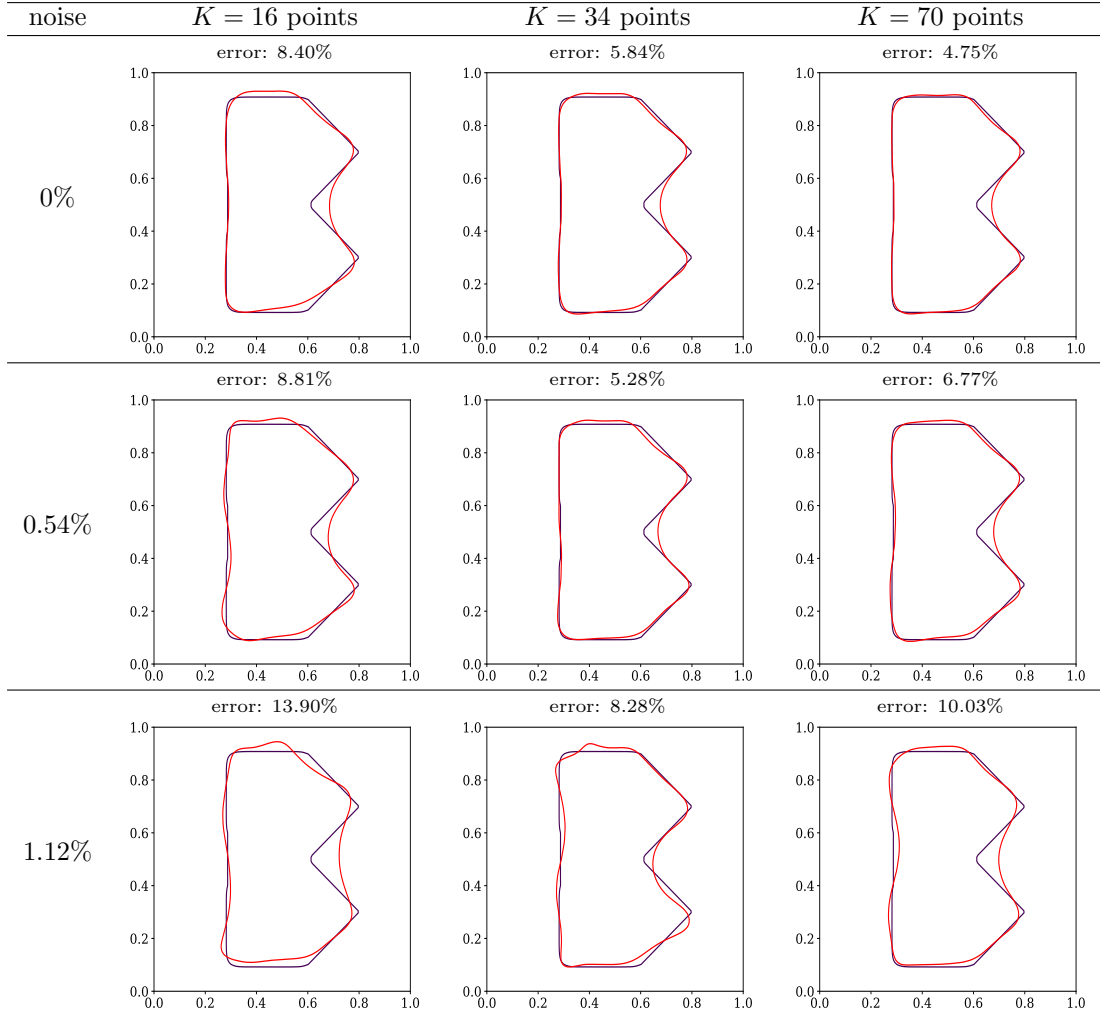


Table 2: Influence of noise and number of point measurements on the reconstruction of a concave shape using $I = 3$ currents (the noise value is the average over the noise values for the three levels of point measurements).

- [2] L. Afraites, M. Dambrine, and D. Kateb. Shape methods for the transmission problem with a single measurement. *Numer. Funct. Anal. Optim.*, 28(5-6):519–551, 2007.
- [3] L. Afraites, M. Dambrine, and D. Kateb. On second order shape optimization methods for electrical impedance tomography. *SIAM J. Control Optim.*, 47(3):1556–1590, 2008.
- [4] M. Alnæs, J. Blechta, J. Hake, A. Johansson, B. Kehlet, A. Logg, C. Richardson, J. Ring, M. Rognes, and G. Wells. The fenics project version 1.5. *Archive of Numerical Software*, 3(100), 2015.
- [5] M. Alsaker, S. J. Hamilton, and A. Hauptmann. A direct D-bar method for partial boundary data electrical impedance tomography with a priori information. *Inverse Probl. Imaging*, 11(3):427–454, 2017.
- [6] H. Ammari, J. Garnier, V. Jugnon, and H. Kang. Stability and resolution analysis for a topological derivative based imaging functional. *SIAM J. Control Optim.*, 50(1):48–76, 2012.
- [7] H. Ammari and H. Kang. *Reconstruction of small inhomogeneities from boundary measurements*, volume 1846 of *Lecture Notes in Mathematics*. Springer-Verlag, Berlin, 2004.
- [8] T. K. Bera. Applications of electrical impedance tomography (EIT): A short review. *IOP Conference Series: Materials Science and Engineering*, 331:012004, mar 2018.

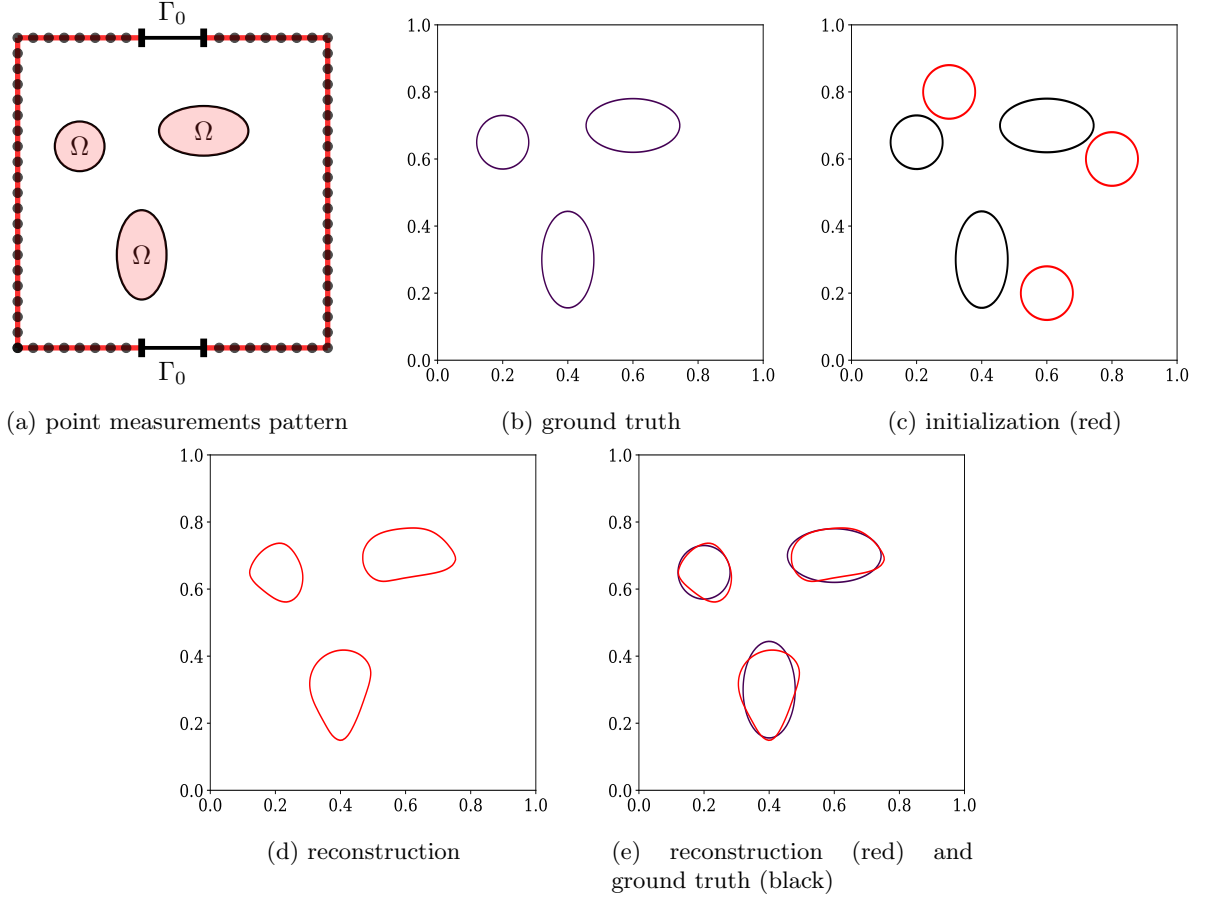


Figure 6: Reconstruction of three ellipses using $I = 7$ currents and $K = 70$ point measurements with 0.63% noise.

- [9] E. Beretta, S. Micheletti, S. Perotto, and M. Santacesaria. Reconstruction of a piecewise constant conductivity on a polygonal partition via shape optimization in EIT. *J. Comput. Phys.*, 353:264–280, 2018.
- [10] M. Berggren. A unified discrete-continuous sensitivity analysis method for shape optimization. In *Applied and numerical partial differential equations*, volume 15 of *Comput. Methods Appl. Sci.*, pages 25–39. Springer, New York, 2010.
- [11] M. Bonnet. Higher-order topological sensitivity for 2-D potential problems. Application to fast identification of inclusions. *Internat. J. Solids Structures*, 46(11-12):2275–2292, 2009.
- [12] L. Borcea. Electrical impedance tomography. *Inverse Problems*, 18(6):R99–R136, 2002.
- [13] L. Borcea, V. Druskin, and A. V. Mamonov. Circular resistor networks for electrical impedance tomography with partial boundary measurements. *Inverse Problems*, 26(4):045010, 30, 2010.
- [14] M. Brühl and M. Hanke. Numerical implementation of two noniterative methods for locating inclusions by impedance tomography. *Inverse Problems*, 16(4):1029–1042, 2000.
- [15] L. Chesnel, N. Hyvönen, and S. Staboulis. Construction of indistinguishable conductivity perturbations for the point electrode model in electrical impedance tomography. *SIAM J. Appl. Math.*, 75(5):2093–2109, 2015.
- [16] E. T. Chung, T. F. Chan, and X.-C. Tai. Electrical impedance tomography using level set representation and total variational regularization. *J. Comput. Phys.*, 205(1):357–372, 2005.

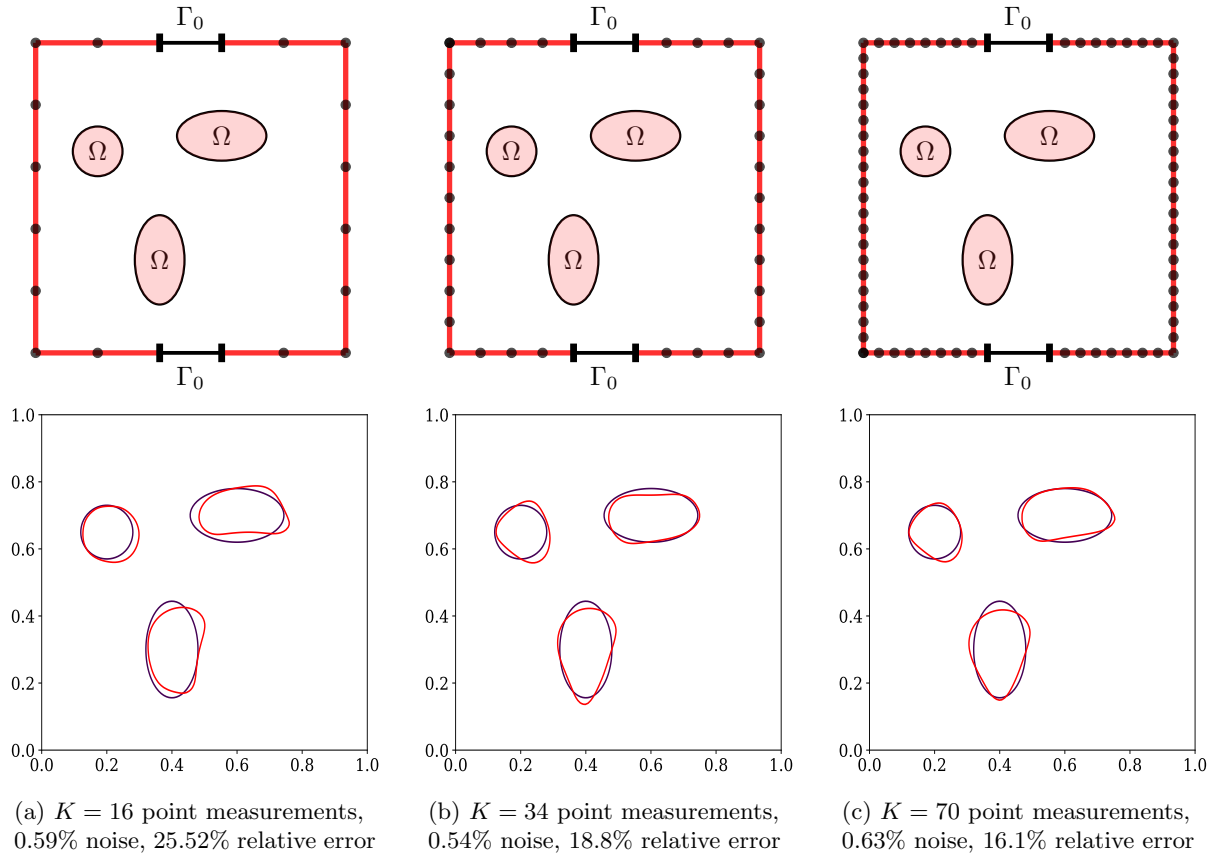


Figure 7: Reconstruction of three ellipses using $I = 7$ currents and different sets of point measurements shown in the first row.

- [17] M. Costabel. On the limit sobolev regularity for Dirichlet and Neumann problems on Lipschitz domains. *Mathematische Nachrichten*, 292(10):2165–2173, June 2019.
- [18] M. Costabel, M. Dauge, and S. Nicaise. Singularities of Maxwell interface problems. *M2AN Math. Model. Numer. Anal.*, 33(3):627–649, 1999.
- [19] T. de Castro Martins, A. K. Sato, F. S. de Moura, E. D. L. B. de Camargo, O. L. Silva, T. B. R. Santos, Z. Zhao, K. Möeller, M. B. P. Amato, J. L. Mueller, R. G. Lima, and M. de Sales Guerra Tsuzuki. A review of electrical impedance tomography in lung applications: Theory and algorithms for absolute images. *Annual Reviews in Control*, May 2019.
- [20] M. Delfour, G. Payre, and J.-P. Zolésio. An optimal triangulation for second-order elliptic problems. *Comput. Methods Appl. Mech. Engrg.*, 50(3):231–261, 1985.
- [21] M. C. Delfour and J.-P. Zolésio. *Shapes and geometries*, volume 22 of *Advances in Design and Control*. Society for Industrial and Applied Mathematics (SIAM), Philadelphia, PA, second edition, 2011. Metrics, analysis, differential calculus, and optimization.
- [22] H. Eckel and R. Kress. Nonlinear integral equations for the inverse electrical impedance problem. *Inverse Problems*, 23(2):475–491, 2007.
- [23] L. C. Evans and R. F. Gariepy. *Measure theory and fine properties of functions*. Studies in Advanced Mathematics. CRC Press, Boca Raton, FL, 1992.
- [24] A. Friedman. Detection of mines by electric measurements. *SIAM J. Appl. Math.*, 47(1):201–212, 1987.

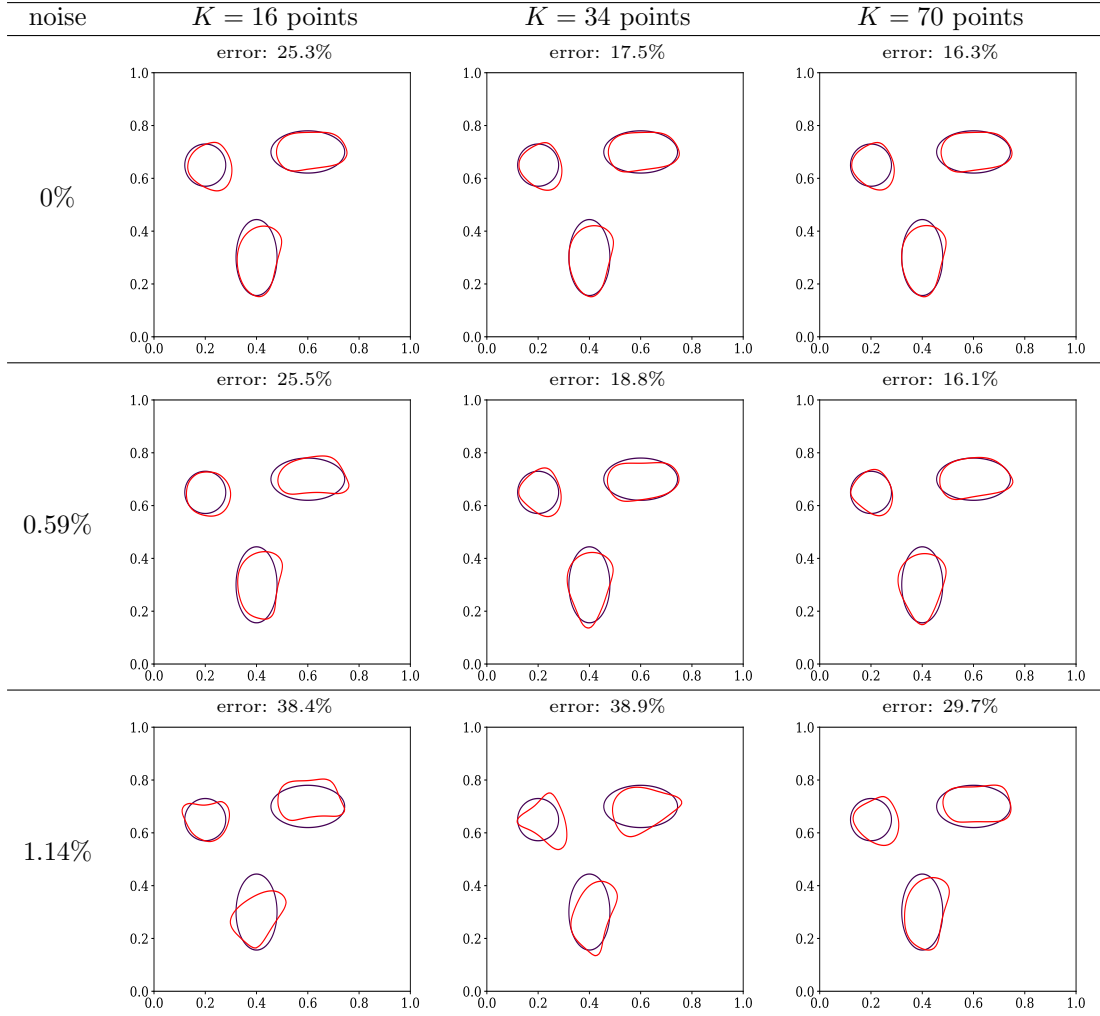


Table 3: Influence of noise and number of point measurements on the reconstruction of three ellipses using $I = 7$ currents (the noise value is the average over the noise values for the three levels of point measurements).

- [25] A. Friedman and V. Isakov. On the uniqueness in the inverse conductivity problem with one measurement. *Indiana Univ. Math. J.*, 38(3):563–579, 1989.
- [26] H. Garde and K. Knudsen. 3D reconstruction for partial data electrical impedance tomography using a sparsity prior. *Discrete Contin. Dyn. Syst.*, (Dynamical systems, differential equations and applications. 10th AIMS Conference. Suppl.):495–504, 2015.
- [27] H. Garde and K. Knudsen. Sparsity prior for electrical impedance tomography with partial data. *Inverse Probl. Sci. Eng.*, 24(3):524–541, 2016.
- [28] H. Garde and S. Staboulis. Convergence and regularization for monotonicity-based shape reconstruction in electrical impedance tomography. *Numer. Math.*, 135(4):1221–1251, 2017.
- [29] M. Giacomini, O. Pantz, and K. Trabelsi. Certified descent algorithm for shape optimization driven by fully-computable *a posteriori* error estimators. *ESAIM Control Optim. Calc. Var.*, 23(3):977–1001, 2017.
- [30] K. Gröger. A $W^{1,p}$ -estimate for solutions to mixed boundary value problems for second order elliptic differential equations. *Math. Ann.*, 283(4):679–687, 1989.

- [31] K. Gröger and J. Rehberg. Resolvent estimates in $W^{-1,p}$ for second order elliptic differential operators in case of mixed boundary conditions. *Math. Ann.*, 285(1):105–113, 1989.
- [32] R. Haller-Dintelmann, C. Meyer, J. Rehberg, and A. Schiela. Hölder continuity and optimal control for nonsmooth elliptic problems. *Appl. Math. Optim.*, 60(3):397–428, 2009.
- [33] M. Hanke, B. Harrach, and N. Hyvönen. Justification of point electrode models in electrical impedance tomography. *Math. Models Methods Appl. Sci.*, 21(6):1395–1413, 2011.
- [34] B. Harrach. Recent progress on the factorization method for electrical impedance tomography. *Comput. Math. Methods Med.*, pages Art. ID 425184, 8, 2013.
- [35] B. Harrach and M. N. Minh. Enhancing residual-based techniques with shape reconstruction features in electrical impedance tomography. *Inverse Problems*, 32(12):125002, 21, 2016.
- [36] B. Harrach and M. Ullrich. Monotonicity-based shape reconstruction in electrical impedance tomography. *SIAM J. Math. Anal.*, 45(6):3382–3403, 2013.
- [37] E. J. Haug, K. K. Choi, and V. Komkov. *Design sensitivity analysis of structural systems*, volume 177 of *Mathematics in Science and Engineering*. Academic Press, Inc., Orlando, FL, 1986.
- [38] A. Hauptmann, M. Santacesaria, and S. Siltanen. Direct inversion from partial-boundary data in electrical impedance tomography. *Inverse Problems*, 33(2):025009, 26, 2017.
- [39] F. Hettlich and W. Rundell. The determination of a discontinuity in a conductivity from a single boundary measurement. *Inverse Problems*, 14(1):67–82, 1998.
- [40] M. Hintermüller and A. Laurain. Electrical impedance tomography: from topology to shape. *Control Cybernet.*, 37(4):913–933, 2008.
- [41] M. Hintermüller, A. Laurain, and A. A. Novotny. Second-order topological expansion for electrical impedance tomography. *Adv. Comput. Math.*, 36(2):235–265, 2012.
- [42] N. Hyvönen. Approximating idealized boundary data of electric impedance tomography by electrode measurements. *Math. Models Methods Appl. Sci.*, 19(7):1185–1202, 2009.
- [43] N. Hyvönen, P. Piironen, and O. Seiskari. Point measurements for a Neumann-to-Dirichlet map and the Calderón problem in the plane. *SIAM J. Math. Anal.*, 44(5):3526–3536, 2012.
- [44] M. Ikehata. How to draw a picture of an unknown inclusion from boundary measurements. Two mathematical inversion algorithms. *J. Inverse Ill-Posed Probl.*, 7(3):255–271, 1999.
- [45] M. Ikehata and S. Siltanen. Numerical method for finding the convex hull of an inclusion in conductivity from boundary measurements. *Inverse Problems*, 16(4):1043–1052, 2000.
- [46] V. Isakov. On uniqueness in the inverse conductivity problem with local data. *Inverse Probl. Imaging*, 1(1):95–105, 2007.
- [47] D. Kalise, K. Kunisch, and K. Sturm. Optimal actuator design based on shape calculus. *Mathematical Models and Methods in Applied Sciences*, 28(13):2667–2717, dec 2018.
- [48] C. Kenig and M. Salo. Recent progress in the Calderón problem with partial data. In *Inverse problems and applications*, volume 615 of *Contemp. Math.*, pages 193–222. Amer. Math. Soc., Providence, RI, 2014.
- [49] C. E. Kenig, J. Sjöstrand, and G. Uhlmann. The Calderón problem with partial data. *Ann. of Math. (2)*, 165(2):567–591, 2007.
- [50] A. Kirsch. Characterization of the shape of a scattering obstacle using the spectral data of the far field operator. *Inverse Problems*, 14(6):1489–1512, 1998.
- [51] K. Knudsen. The Calderón problem with partial data for less smooth conductivities. *Comm. Partial Differential Equations*, 31(1-3):57–71, 2006.

- [52] K. Krupchyk and G. Uhlmann. The Calderón problem with partial data for conductivities with $3/2$ derivatives. *Comm. Math. Phys.*, 348(1):185–219, 2016.
- [53] H. Langtangen and A. Logg. *Solving PDEs in Python: The FEniCS Tutorial I*. Simula SpringerBriefs on Computing. Springer International Publishing, 2017.
- [54] A. Laurain and K. Sturm. Distributed shape derivative *via* averaged adjoint method and applications. *ESAIM Math. Model. Numer. Anal.*, 50(4):1241–1267, 2016.
- [55] A. Logg, K.-A. Mardal, and G. N. Wells, editors. *Automated Solution of Differential Equations by the Finite Element Method*, volume 84 of *Lecture Notes in Computational Science and Engineering*. Springer, 2012.
- [56] S. Nicaise and A.-M. Sändig. General interface problems. I, II. *Math. Methods Appl. Sci.*, 17(6):395–429, 431–450, 1994.
- [57] J. Sokółowski and J.-P. Zolésio. *Introduction to shape optimization*, volume 16 of *Springer Series in Computational Mathematics*. Springer-Verlag, Berlin, 1992. Shape sensitivity analysis.
- [58] E. Somersalo, M. Cheney, and D. Isaacson. Existence and uniqueness for electrode models for electric current computed tomography. *SIAM J. Appl. Math.*, 52(4):1023–1040, 1992.
- [59] K. Sturm. *On shape optimization with non-linear partial differential equations*. PhD thesis, Technische Universität Berlin, October 2014.
- [60] K. Sturm. Minimax lagrangian approach to the differentiability of nonlinear pde constrained shape functions without saddle point assumption. *SIAM Journal on Control and Optimization*, 53(4):2017–2039, 2015.
- [61] K. Sturm. Shape optimization with nonsmooth cost functions: from theory to numerics. *SIAM J. Control Optim.*, 54(6):3319–3346, 2016.
- [62] F. Tröltzsch. *Optimal control of partial differential equations*, volume 112 of *Graduate Studies in Mathematics*. American Mathematical Society, Providence, RI, 2010. Theory, methods and applications, Translated from the 2005 German original by Jürgen Sprekels.
- [63] J. Virieux and S. Operto. An overview of full-waveform inversion in exploration geophysics. *GEO-PHYSICS*, 74(6):WCC1–WCC26, Nov. 2009.
- [64] W. P. Ziemer. *Weakly Differentiable Functions*. Springer New York, 1989.